MOUNTAIN-PLAINS CONSORTIUM

MPC 17-335 | S. Pei, N. Wehbe, and B. Ahrenstorff

Evaluation of Ice Loads on Bridge Sub-Structures in South Dakota

MOUNTAIN-PLAINS CONSORTIUM REGION 8

A University Transportation Center sponsored by the U.S. Department of Transportation serving the Mountain-Plains Region. Consortium members:

Colorado State University
North Dakota State University
South Dakota State University
University of Colorado Denver
University of Denver
University of Utah
Utah State University
University of Wyoming

EVALUATION OF ICE LOADS ON BRIDGE SUB-STRUCTURES IN SOUTH DAKOTA

Shiling Pei
Assistant Professor
Department of Civil and Environmental Engineering
Colorado School of Mines
Golden, CO 80401
Phone: (303) 273-3932
Email: spei@mines.edu

Nadim I. Wehbe
Professor and Department Head
Department of Civil and Environmental Engineering
South Dakota State University
Brooking, SD 57007
Phone: (605) 688-5427
Email: nadim.wehbe@sdstate.edu

Brittney Ahrenstorff
Structural Engineer
Kiewit Corporation

October 2017

Acknowledgment

The authors would like to acknowledge the financial support of the Mountain-Plains Consortium (MPC) and the South Dakota Department of Transportation for funding this study through project MPC-400.

Disclaimer

ABSTRACT

A research study was conducted by South Dakota State University in cooperation with the South Dakota Department of Transportation (SDDOT) to assess applicability of the American Association of State Highway and Transportation Officials (AASHTO) design calculations for the dynamic ice loads on bridge structures in South Dakota. Ice loads were measured at two sites for two consecutive winters (2013 and 2014) using a monitoring system designed and tested in the J. Lohr Structures Lab at SDSU. Sites were selected based on previous ice thickness and strength measurements, water level heights during spring thaw, feasibility of installation, and discussion with SDDOT personnel. The recorded data were analyzed using statistical approaches to develop a probabilistic model of ice impact load level for each site. Distribution of the maximum ice load for both sites over a 75-year period was estimated. Based on these extreme ice load statistics, reliability indices were determined for the AASHTO formula ice load values. The reliability index showed that current load calculations adopted by SDDOT ensure a reasonably high reliability index for both sites based on the two years of data collected during the study. A recommendation was made regarding the calculation of small-stream ice load in South Dakota using the AASHTO formula. Additional data collection was also recommended for future studies.

TABLE OF CONTENTS

LIST OF TABLES

LIST OF FIGURES

LIST OF ACRONYMS

AASHTO	American Association of State Highway and Transportation Officials
CDF	Cumulative Distribution Function
FHWA	Federal Highway Administration
HSS	Hollow Structural Section
LRFD	Load and Resistance Factor Design
PVC	Polyvinyl Chloride
SDDOT	South Dakota Department of Transportation
SDSU	South Dakota State University
USGS	United States Geological Survey

EXECUTIVE SUMMARY

A research study was conducted by South Dakota State University in cooperation with the South Dakota Department of Transportation (SDDOT) to assess applicability of the American Association of State Highway and Transportation Officials (AASHTO) design specifications for dynamic ice loads on bridge sub-structures in the state of South Dakota.

The research study comprised four major activities, the first was development of an ice loading monitoring system. The monitoring system designed in this study was unique in that it measured the ice impact force explicitly through a one-foot diameter hollow structural section (HSS) pipe load transducer installed at the upstream direction of the bridge pier. Based on fundamental force equilibrium, the configuration included an HSS pipe spanning two strain-gauge instrumented load cell supports with overhang. The system was designed to be robust enough to remain elastic under 400 kips ice impact load at any location, be able to be attached to bridge piers and partially submerged under water, and operate continuously during harsh winter conditions. The strain gauge load cells were assembled and calibrated in SDSU's Structure's Lab to ensure reliability of the collected data. The monitoring system also had 14-channel data acquisition capacity with a 5-Hz sampling rate, designed to record 12 channels of strain measurement data and two channels of temperature data. The entire system was powered by a solar panel and battery, and could be monitored using a wireless modem.

The second activity involved selection of the study sites and installation of the monitoring system at each site. Working collaboratively with the project's technical panel and other SDDOT personnel, two small stream sites were selected based on accessibility, installation feasibility, and ice characteristics from former research on ice strength and thickness. The US14 site over the James River site was selected because it was identified in a previous USGS study as the location where the highest ice strength was measured. The I-29 site over the Big Sioux River is close to Brookings, South Dakota, which is a typical small stream situation with potentially high ice impact loads. The research team and project panel also considered some other sites that may have experienced ice dam conditions. Those sites were not selected because of the difficulty caused by a large water level variation. As the first study of its kind on a stream in the United States, the two sites selected were reasonable. Although these sites do not represent ice dam conditions (likely the worst case scenario for small-stream lateral ice loads), the scope of the study is appropriate considering the current state of knowledge on small-stream ice loads. Installation of the devices on the selected sites was completed in November 2012, with a great deal of assistance from SDDOT personnel and project panel members.

Collecting data from the ice load monitoring system was this study's third activity. The automatically collected data included strain gauge and temperature data at a 5-Hz sampling frequency. Data were recorded on data logger memory cards and periodically (approximately monthly) transferred to a lab computer for post processing. The data collection was only active during the winter period, approximately from December to April. When there was no ice in the waterway, data were not collected. Data collection continued for two winter seasons—2013 and 2014. In addition to ice load data collection, several measurements of ice thickness and ice compressive strength were conducted during the monitoring period.

The fourth study activity was analysis of data acquired by the ice load monitoring system. After two years of ice load data collection, the research group identified (after processing the raw data, details presented in this report) about 60,000 ice impact events for the James River site, with a maximum recorded ice load of about 190 kips. Close to 10,000 ice impact events for the Big Sioux River site also were identified, with a maximum recorded ice load of about 60 kips. Considering these data are only from two years of collection, the suitable design ice load for a bridge's design life—typically 75 years—must be derived

from the theory of probability and reliability. In this study, researchers first established probabilistic distribution of single ice impact load values as a lognormal distribution, and then projected the single impact event cumulative distribution function (CDF) to 75-year maximum impact event CDF by assuming independence of the ice impact events. The average annual impact count was also estimated for both sites based on the measured data. The statistical median value of the maximum ice impact load in 75 years was 175 kips for the James River site and 82 kips for the Big Sioux River site.

Once the 75-year maximum impact load distributions were obtained for both sites, the AASHTO ice load formula was used to calculate design ice load for the cross-section size of the monitoring system. Reliability of the calculated design load levels under different ice strength and reduction options was determined. The following two main recommendations were developed based on the objective of maintaining a minimal reliability index of 3.0 considering the load uncertainty alone.

For flows similar to the James and the Big Sioux rivers, we recommend that SDDOT use an effective ice strength of 32 ksf for small streams, as listed in AASHTO LRFD Bridge Design Specifications, and obtain ice thickness from the ice thickness map contained in the SDDOT report "Estimation of Ice Thickness and Strength for Determination of Lateral Ice Loads on Bridge Substructures in South Dakota SD98-04-F." We also recommend that SDDOT should not consider the small stream reduction factor given in the AASHTO LRFD Bridge Design Specifications when calculating ice loads for flows similar to those that form on the James and the Big Sioux rivers.

These recommendations are based on the fact that using the ice thickness map data and 32 ksf effective ice strength together with the AASHTO LRFD Bridge Design Specifications requirements will generate design ice load values that result in a reliability index greater than 3.0 for both sites. Reliability index is a numerical value reflecting the probability of designing ice load value being greater than real ice load during the design life of the structure. It is calculated by inputting the aforementioned probability into the inverse standard Normal cumulative distribution function (CDF). This recommendation is based on the comparison between the AASHTO load calculation and the extreme ice load statistics derived from two-year monitoring data at the two selected sites. Although data are limited, the research team believes that the recommendation is on the safe side of AASHTO recommendations and is supported by existing data with reasonable reliability. The exclusion of ice dams and the limitation to small streams is in place because of the nature of the monitoring sites where data were generated.

The S.D. Department of Transportation should commission work to redesign the ice load monitoring system and collect data for at least five years from river sites that may induce more critical ice load conditions. This recommendation is contingent upon the need to conduct a comprehensive ice load calibration for South Dakota rivers. If there is no immediate need, this recommendation will not be applicable. If there is a need to perform this calibration, we recommend that SDDOT consider the possibility of conducting more data collection on ice impact load for a longer period of time (preferably more than five years) and at sites that cover more critical conditions (such as thick ice sheet floats and ice dams). The potential benefit of conducting this work is to develop an understanding of the realistic ice load demands in these locations and eventually correlate the ice load with weather and geographical data in South Dakota, and develop a viable and scalable procedure for river ice load monitoring. Ideally the sites where ice impact damage was observed on bridge structures should be included. Based on experience from this project, the following modifications of the study plan should be implemented:

- Redesign the monitoring system with a focus on its sensitivity to long term temperature variations in an as-installed configuration (rather than only relying on the laboratory testing and calibration).
- Conduct the study in two phases. The first phase will only conduct field trial at limited sites, collect data for 1 to 2 years, and adjust the design based on shortcomings of the initial monitoring

system observed during the first phase to increase its robustness and accuracy. The second phase will then replicate the validated system at multiple sites and collect data for a longer period (5 to 10 years).

- Supplement the ice load measurement with visual data, preferably using remote cameras to link the measurements with images reflecting river conditions.
- Seek collaboration with other research entities that have capacity to conduct scaled modeling or ice floe characterization, such as the US Army Cold Regions Research and Engineering Lab. Such collaboration was not pursued during this first phase of the study.

With the experience gathered and lessons learned from this study, it is likely that researchers can improve the current design and obtain better ice load data.

1. INTRODUCTION

1.1 Project Description

Ice loads on a bridge structure can be one of the major components for Extreme Limit State combinations specified in the AASHTO Code. In seismically inactive regions such as South Dakota, ice loads can be the predominant lateral load in the design of bridge sub-structures. Accurate estimation of the magnitude of ice forces that act on bridge piers in northern climates is critical in the design of new bridges and in evaluation of existing bridges. While the AASHTO Code provides empirical equations to calculate the design of ice loads based on effective ice strength and thickness, these formulas were developed assuming thick ice formation that often is quite different from the relatively smaller chunks of ice floe (i.e. not a large complete ice sheet, size relative to dimension of bridge piers) that form on South Dakota rivers. Even with accurate ice strength and thickness values, ice loads calculated based on AASHTO formulas may be inaccurate because boundary conditions and ice breaking conditions may not be ideal as assumed. Using these load levels in design may lead to over-designed bridge sub-structures with excessive construction cost, or under-designed bridge sub-structures that may negatively affect public safety.

As a commonly encountered phenomenon in cold regions, the mechanism of ice formation in natural water bodies and ice loads on bridge sub-structures had been studied for decades. Accurate prediction of extreme lateral ice loads on supporting structural elements at water level is of special interest to researchers due to its implications on structural design. A variety of methods was employed in ice load estimation, including mechanistic modeling of the ice-structure interaction using nonlinear finite element models (e.g., Ahmed 1994, Yuan 2009), scaled testing in a hydraulic laboratory (e.g., Timco 1995, Lever 2001, Jochmann 2003), and field monitoring on full scale structures (e.g., Frederking 1992, Brown 2010). In these studies, several factors were believed to have significant influence on ice loads, including geometry of the sub-structure, ice thickness and strength, and ice failure mode. A notable long term ice load monitoring project was the Confederation Bridge pier ice load monitoring project in Canada, in which ice loads on three of the bridge piers were continuously monitored for more than 11 years after the bridge first opened in 1998. The monitoring system consisted of multiple pressure panels installed to the sub-structure, and tiltmeters and accelerometers. A significant observation from these field monitoring projects was that the actual ice load was much smaller than what had been used in the design of these structures. However, most of these studies were conducted for ice load in an ocean water environment. There has not been any notable full-scale experimental study on river ice load estimation in the United States.

During 1998-2002, the U.S. Geological Survey (USGS), in cooperation with SDDOT, conducted a study to evaluate factors affecting ice forces at selected bridges in South Dakota. The study gathered a significant amount of ice thickness and strength data from six sites representative of South Dakota river conditions. The study also recommended an Accumulative Freezing Degree Day equation for ice thickness estimation in South Dakota. However, the measured ice crushing strength from the study had large variability and could result in an extremely large ice load if used directly in the AASHTO formula. After the study, an equivalent ice strength of 250 lb/in^2 was used for South Dakota bridge design using the AASHTO formula, with the actual ice load level remaining largely unknown. This knowledge gap provided the impetus for the current study to conduct direct ice load measurements and estimate bridge sub-structure ice load during the time of maximum ice-crushing strength in mid- to late winter and during ice breakup in early spring.

1.2 Objectives

This study focused on monitoring ice loads directly at bridge sites in South Dakota and comparing measured load statistics with codified design load values. The research sought to provide bridge designers realistic and relevant ice load information for small streams in South Dakota. The research objectives for this study included:

- Developing an efficient and accurate ice load monitoring system for bridge sub-structures in cold regions.
- Accurately determining ice loads exerted on bridge sub-structures through continuous monitoring of ice load at selected sites in South Dakota.
- Evaluating applicability of AASHTO equations based on observed ice loads on South Dakota bridges and providing a recommendation for the application of the AASHTO ice load section for bridge design in South Dakota small streams.

1.3 Literature Review

This section describes significant studies in the past related to the subject of this research. First, several other studies that relate to ice load calculation and monitoring are discussed. Then, a study completed by the U.S. Geological Survey (USGS) on thickness and strength of ice in South Dakota is introduced (Niehus, 2002). Finally, the AASHTO (2014) equations and current ice load design practices for South Dakota are discussed.

1.3.1 Field and Experimental Studies

Many studies in the past looked at ice formation and break-up processes in waterways. Other studies focused more on the effects of the ice loads on bridge structures and how to account for them in design. These studies have added to the slim body of knowledge related to the dynamic ice forces on bridge piers and their effects.

Ice formation varies across the globe and ice will have different properties based on the process. In South Dakota, much of the ice is formed from snow accumulation. In the paper titled “River and Lake Processes Relevant to Ice Loads,” Robert Gerard discusses the important influence that snow accumulation has on ice thickness. First the snow insulates ice cover and reduces growth rate. But once the snow depth is about half the ice thickness, the weight of the snow will submerge ice cover. When this happens, water floods through the cracks and saturates lower layers of snow. This continues until the saturated snow layer freezes, forming snow ice (Gerard, R. 1983). This type of ice formation mechanism will produce ice that has more air content and is more fragmented, which is different from the thick solid ice formations assumed by much of the design codes used today. Therefore, properties of the ice may be different in South Dakota compared to other regions. This is one important factor to consider when designing bridges for the state.

Another important topic for discussion is the ice floe failure types. Five types of failure are commonly seen when a moving ice floe strikes a bridge pier. The type of failure that occurs is influenced by strength of the ice, geometry of the pier, and size of the floe. Montgomery et al. (1984) describe the following five types of ice failure:

- Crushing—The ice fails by local crushing across the width of the pier. Crushed ice is continually cleared from a zone around the pier as the floe moves past.

- Bending—For piers with inclined noses, a vertical reaction component acts on the impinging ice floe. This reaction causes the floe to rise up the pier nose and fail as flexural cracks form.
- Splitting—When a comparatively small floe strikes a pier, stress cracks split the floe into smaller parts.
- Impact—If the floe is small, it is brought to a halt when impinging on the nose of the pier by bending or by splitting.
- Buckling—For very wide piers, where a large floe cannot clear the pier as it fails, compressive forces cause the floe to fail by buckling in front of the pier nose.

Montgomery et al. (1984) also stated that the controlling design dynamic ice forces on typical bridge piers on larger bodies of water will be caused by crushing and bending ice failures. However, impact failures could be the controlling force for bridges on smaller streams not capable of carrying large ice floes. Due to the high uncertainty in ice formation and characteristics, criteria based on actual field measurements (Haynes et al. 1991) must be developed for the design of bridges under ice loads. These measurements are made at existing bridges to refine the design loads for future designs. To date, there have been only a handful of papers written about direct measurements studies (Haynes et al. 1991; Brown et al. 2009). With most of these studies conducted for bridges over straits and ocean water, there is a lack of studies on inland rivers and streams. There was no study completed previously in South Dakota.

1.3.2 USGS – SDDOT Study of Ice Thickness and Ice-Crushing Strength

A study completed by the U.S. Geological Survey (USGS), in cooperation with the SDDOT, led directly to this research project. The previous study was titled "Estimation of Ice Thickness and Strength for Determination of Lateral Ice Loads on Bridge Substructures in South Dakota" and was written by Colin A. Niehus. This study was performed because of the importance of estimating the magnitude of ice forces that act on bridge piers and abutments in northern climates (Niehus, 2002). Niehus states that ice load evaluation is complex because ice forces acting on bridges tend to be related to many factors, including ice thickness, ice-crushing strength, water depth, stream-flow, and wind. Ice thickness and ice-crushing strength are the most important factors that go into the design equations for estimation of the dynamic ice forces. The estimation of these factors for use in design and evaluation in the state of South Dakota was the primary objective of Niehus's study.

Niehus and his research team measured ice thickness and ice-crushing strength at six sites across South Dakota from February 1999 to April 2001. They developed a map that gives the estimated maximum potential ice thickness for regions across the state.

The ice-crushing strength measurements were used to estimate an appropriate design value. The measurements showed that it would be practical to assume that sites across South Dakota could potentially develop ice with strength of 1,000 psi during the coldest part of the winter, if the most extreme conditions were present. Niehus determined that it was more likely that the ice-crushing strength during the spring thaw/breakup would be much lower than 1,000 psi. Data they collected closer to spring thaw indicated that 250 psi was an appropriate value to use in estimating ice forces. Therefore, using the maximum ice strength of 1,000 psi would grossly over-estimate the ice forces.

In the conclusions and considerations for implementation section of the aforementioned study, the author recommended direct measurement of ice forces acting on bridge structures for South Dakota bridge design practice. This provided the impetus for this study.

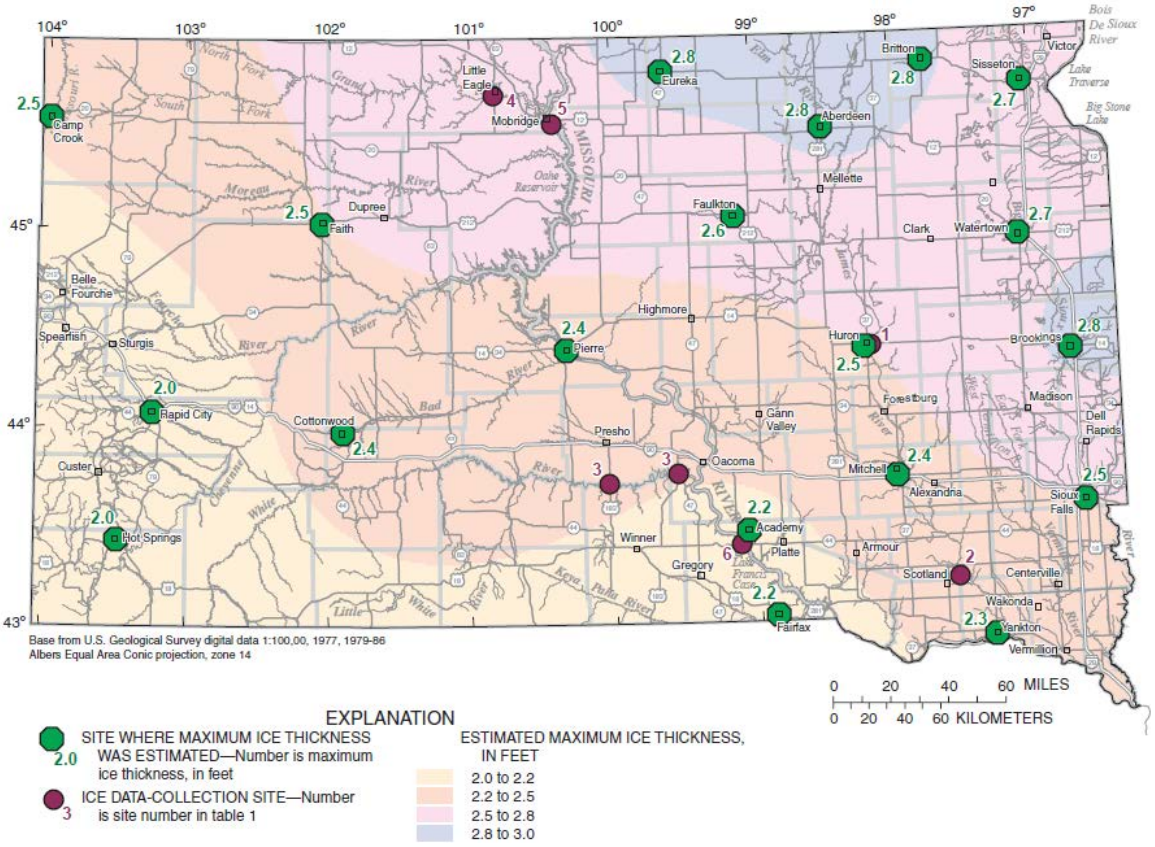

Figure 1.1 Estimated Maximum Potential Ice Thickness for Waterways in SD (Niehus, 2002)

1.3.3 South Dakota Current Practices and AASHTO Equation

Practices followed in South Dakota for bridge design have developed over time based on changing codes and updated knowledge and information. The previously discussed study completed by the USGS in cooperation with the SDDOT caused a change in values used by SDDOT bridge engineers when designing for ice loads. Before that study was completed, engineers assumed that effective ice-crushing strength (as defined by AASHTO LRFD Bridge Design Specifications equations) for the state during breakup was 100 psi. This was determined to be too low when compared to data collected in Niehus' study. Therefore, this value was increased to 250 psi for the state (which is equivalent to the 36 ksf value recommended in AASHTO LRFD). The study also resulted in a map of the state of South Dakota with estimated maximum potential ice thickness regions across the state ranging from 2 to 3 feet. The AASHTO (2014) equations used by SDDOT for determining ice loads (AASHTO Section 3.9.2-Dynamic Ice Forces on Piers) require values for the ice-crushing strength and the ice thickness.

Only bridges with no inclination to their piers will be discussed here. Ice forces on bridges that have inclined piers are determined using other considerations that can be found in Section 3.9.2 of the AASHTO specifications (AASHTO, 2014). For piers that are not inclined, the horizontal ice force, F_c, caused by ice floes that fail by crushing over the full width of the pier is the design ice force. F_c is given by AASHTO Equation 3.9.2.2-1 as follows:

$$F_c = C_a\, p\, t\, w \qquad \textbf{Equation 1.1}$$

Where

F_c = design ice crushing force (kips)

C_a is a coefficient accounting for the effect of the pier width/ice thickness ratio where the floe fails by crushing. C_a is given as:

$$C_a = \left(\frac{5\,t}{w} + 1 \right)^{0.5}$$

p = effective ice crushing strength (ksf)

t = thickness of ice (ft)

w = pier width at level of ice action (ft)

The code gives values for effective ice crushing strength to be used in the absence of more precise information. These values and their respective ice conditions are given below.

- 8.0 ksf (55.6 psi), where breakup occurs at melting temperatures and the ice structure is substantially disintegrated;
- 16.0 ksf (111 psi), where breakup occurs at melting temperatures and the ice structure is somewhat disintegrated;
- 24.0 ksf (166.7 psi), where breakup or major ice movement occurs at melting temperatures, but the ice moves in large pieces and is internally sound; and
- 32.0 ksf (222 psi), where breakup or major ice movement occurs when the ice temperature, averaged over its depth, is measurably below the melting point

These values are all lower than the 250 psi recommendation made by the USGS-SDDOT study discussed previously. AASHTO (2014) allows a designer to reduce the overall design force for small streams (Section 3.9.2.3 of the code). According to AASHTO, for small streams not conducive to the formation of large ice floes, consideration may be given to reducing the forces determined in Section 3.9.2.2, but under no circumstances shall the forces be reduced by more than 50%. The ice load reduction factor, K1, is given in Table C3.9.2.3-1 of the AASHTO LRFD (Load and Resistance Factor Design) specifications (AASHTO, 2014) and is reproduced in Table 1.1. K_1 is dependent on the ratio A/r^2 where A is defined as the plane area of the largest ice floe (in units of ft^2) and r is the radius of the pier nose (in units of feet). This reduction is meant for the small stream situation where the ice floes fail by the impact mode instead of crushing. This reduction factor is currently considered for small streams in South Dakota.

Table 1.1 Reduction Factor K_1 for Small Streams

A/r^2	**Reduction Factor, K_1**
1000	1.0
500	0.9
200	0.7
100	0.6
50	0.5

Using the design parameter of pier width=2.5 feet and ice thickness= 2 feet, the AASHTO ice load equation will result in an ice load that varies from 67 kips to 270 kips (depending on the effective ice crushing strength value used (a range of 8 to 32 psf was given in AASHTO). This showed a wide range of variability for the calculated ice loads even when the values for the ice thickness and pier width are given. Furthermore, the ice loads could be reduced by up to 50% as discussed previously. This situation makes the design for ice load difficult. In South Dakota DOT bridge design practices before the Niehus study, an assumed ice load level of 10 kips per foot of substructure width in the transverse direction has been used. Using this criteria, a 2.5-foot-wide bridge pier would result in a design ice load equals to 25 kips. Following the measured ice crushing strength measured in the Niehus study (250 psi), the design load in the same example calculated using the AASHTO design code formula with the ice thickness equals to 2.0 feet will be 425 kips. This value could be reduced by up to 50% using engineering judgment. These different options and assumptions in design load calculation can cause a large variability in bridge pier lateral design. This study was conducted to provide data to support more reasonable design ice load estimation for South Dakota streams.

2. ICE LOAD MONITORING DEVICE

2.1 Design of Ice load Monitoring System

2.1.1 Conceptual Design

Development of the monitoring system required consideration of several key factors including designing the column's attachment system, determining the shape and load path that would yield best results while maintaining an economic design, and determining how to protect sensitive pieces in the system from damage. Multiple design options were conceptualized and assessed. The overall design concept was to measure the dynamic ice loads directly by installing a monitoring system onto the bridge pier at each of the selected sites.

The selected concept can be modeled as a beam that has a simply supported segment between two load cells and a cantilever segment that will receive the ice load as shown in Figure 2.1. The design uses a round HSS section as the load transducer. The force from an impact is transferred from the transducer through load cells and then into the column. Figure 2.1 shows the ice impact force, P, applied to the transducer can be calculated as shown in Equation 2.1:

$$P=F_2-F_1 \qquad \text{Equation 2.2}$$

Where F_1 and F_2 are the magnitude of the forces at the supports (where load cells were installed) in the direction shown.

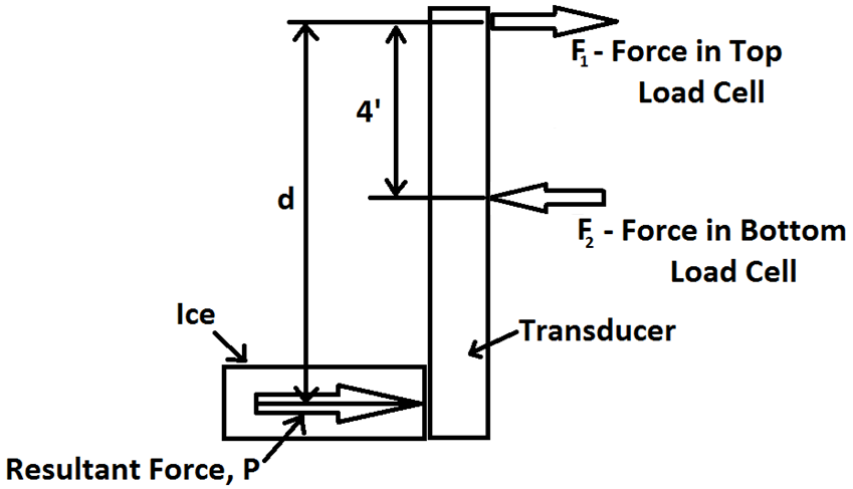

Figure 2.2 Conceptual Monitoring System Configuration

2.1.2 Structural Design of the Monitoring System

The design for the data acquisition system consisted of several components assembled together and attached to the bridge pier. This section discusses the mechanical components that were consistent at both sites. Figure 2.2 shows a 3D rendering of the system, together with the basic dimensions of this monitoring system.

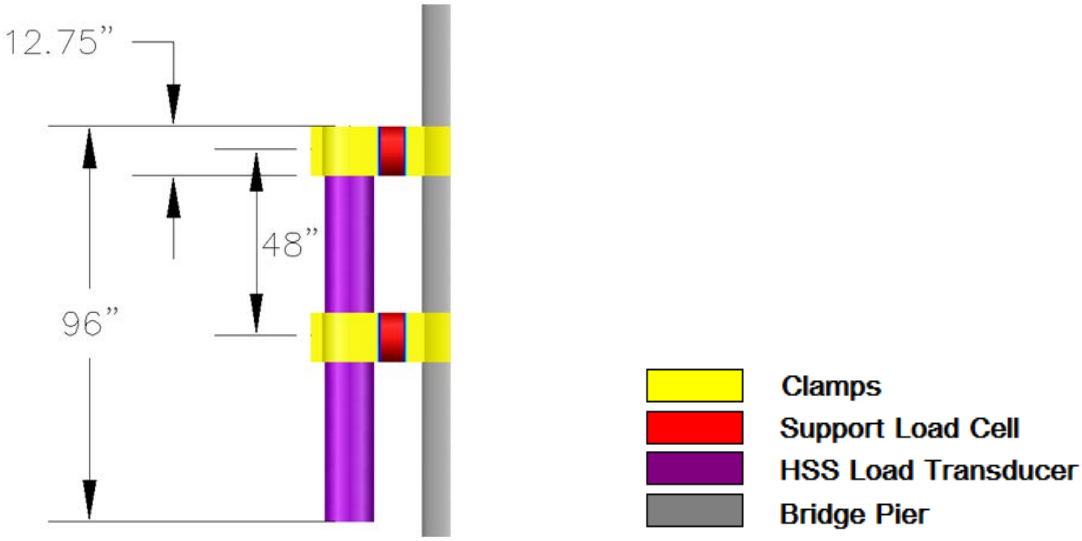

Figure 2.3 System Rendering

The main component of this system is the eight-foot hollow structural section (round HSS 12.75” OD x 0.5” wall thickness) that was used as the transducer. This piece receives impacts and then transfers load into supports referred to as load cells. Each load cell consists of several smaller pieces welded together to form the composite piece. Figure 2.3 shows the assembled load cell. The transducer pipe was connected to the load cells using clamps that were fabricated using ¼” A36 steel plates bent into shape with ¼” A36 steel stiffeners welded to the outer flanges. The clamps connected to one another and to the load cells using 7/8” threaded rods that were tightened on each side using heavy hex head nuts with flat washers and lock washers to create a secure connection.

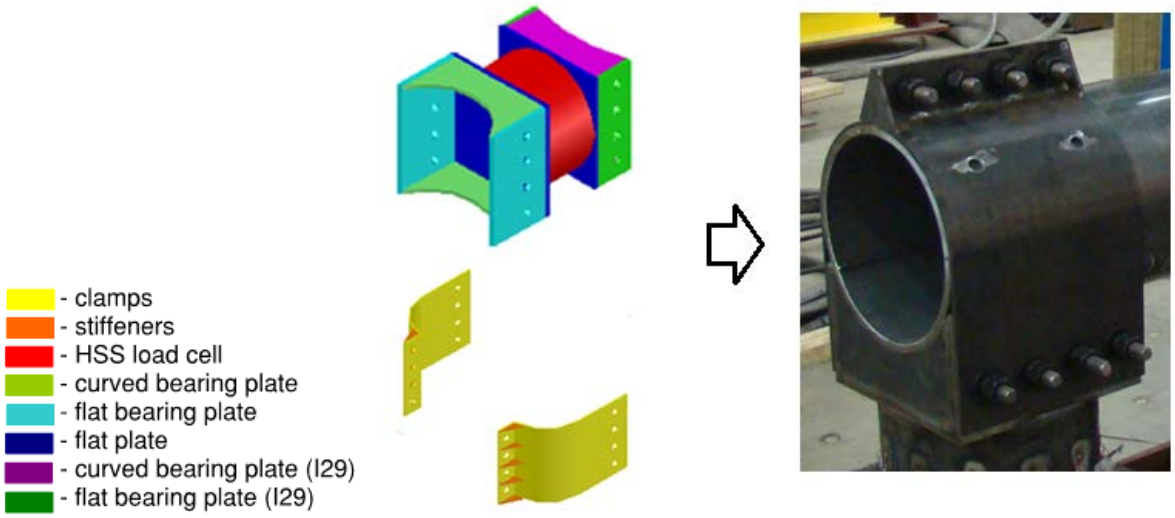

Figure 2.4 Custom Built Load Cell for the Monitoring System

2.1.3 Data Acquisition System

The data acquisition system consisted of strain gages connected to a data logger, a cellular modem with antenna, a solar panel, and a battery. A diagram of the assembly is shown in Figure 2.4. A photovoltaic controller was used to connect the power (solar panel and battery) to the load (data logger and cell modem).

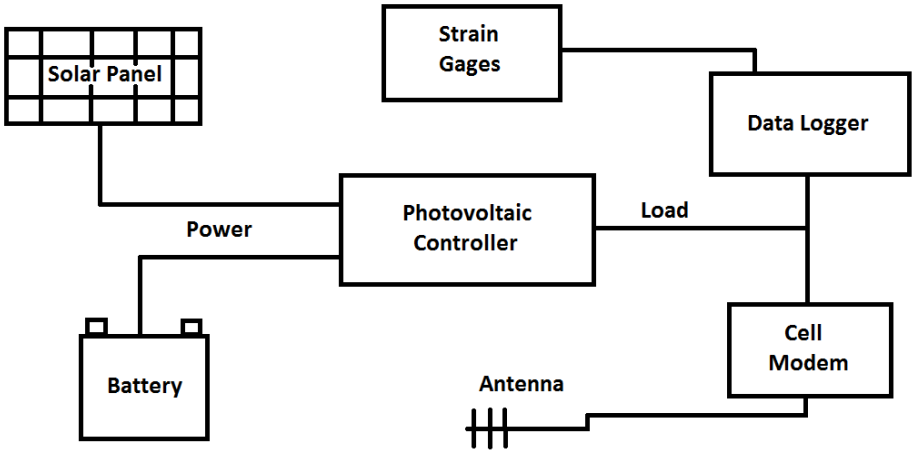

Figure 2.5 Diagram of Electronic System

The data logger used for this project was a Campbell Scientific CR3000 Micrologger. At each site, the data logger was connected to 12 strain gages and two thermocouples that collected data at a 5 Hertz sampling rate. Data were collected and stored on memory cards inserted in the data logger. The memory cards were retrieved frequently and switched. The capacity of the data logger's internal memory allowed the memory cards to be switched without losing data. A photo of the data logger used is shown in Figure 2.5. The strain gauges and thermocouples were connected to the data logger using 18 AWG shielded tray cable. These cables had PVC jackets and three conductors. Each cable at the James River site was about 130 feet long, and the cable was about 150 feet long at the I-29 site. A quarter bridge circuit was used to connect each strain gage cable to the data logger. A program created using Campbell Scientific's RTDAQ computer software was used to run the data logger. This program was also used to convert data into a usable form once collected.

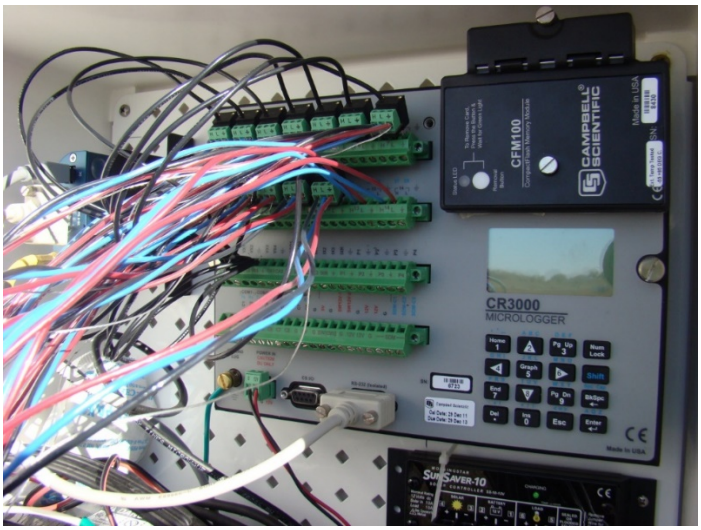

Figure 2.6 CR3000 Data Logger used in the project

A cellular modem was connected to the data logger. The antenna was mounted on the side of the bridge at the I-29 site, while a directional antenna was attached to the solar panel post at the James River site. The modem was used to communicate with the data loggers remotely. Status of the system was checked frequently via this connection. Real-time data could be collected to monitor activity at the site, if desired. Files stored on the memory cards were too large to collect remotely. A photograph of the cellular modem and the solar panel used on this project to charge the battery that powers the system is shown in Figure 2.6.

Figure 2.7 Wireless Transmission Modem and Solar Panel Remote Power

The data logger, cell modem, battery, and photovoltaic controller were housed in a Campbell Scientific weatherproof box attached to the solar panel pole at the James River site and mounted beneath the bridge on the southern abutment at I-29.

Strain gages were the primary sensor used in this system. The strain was measured for each of the load cells and was later converted to forces that were used to determine the magnitude of the applied load. The gages used were 350-ohm universal general-purpose strain gages with an exposed solder tab area. They had a workable temperature range of -100 degrees to 350 degrees Fahrenheit. Twelve gages were applied to each load cell. They were located equidistant from one another around the outside of the circular section in the middle as shown in Figure 2.7.

F**igure 2.8** Strain Gages Applied in the Center of the HSS Load Cell

Thermocouples were also applied to the load cells. Each load cell had a thermocouple attached to the middle of the HSS section near the strain gages. The thermocouples were connected to the data logger and collected data at the same rate as the strain gages (5 Hertz) to collect temperature information. Two thermocouples (one on each load cell) were necessary due to the possibility that the bottom load cell became submerged while the top load cell remained in the open air, causing a potential temperature differential between the two.

2.1.4 Impact Protection

The monitoring system was partially submerged during the monitoring period and was susceptible to impacts from ice and debris. Proper protection was critical not only for the gages, but also for cables that led from the gages to the data logger.

Several protection measures were used to prevent damage and maintain integrity of the collection equipment. The first layer of protection was applied to the gages themselves. After short lead wires were soldered to the placed gages, two layers of protection were applied. The bottom layer was a microcrystalline wax that was used as a water-immersion coating to protect the gages from getting wet. The top layer was a two-part polysulfide liquid polymer compound. This layer also resisted moisture, but was mainly used for mechanical protection. Once cured, the liquid polymer provided a tough barrier to protect the gages against any debris or ice. Figure 2.8 shows a load cell with the strain gage protection barrier circled. The top layer of liquid polymer is visible.

Figure 2.9 Load Cell with the Strain Gage Protection (Highlighted)

After the system was installed on site, the outer protection components were placed. The short cables that connected to the strain and temperature gages on one end and to the long shielded cabling on the other were run through the inside of plastic tubing that was filled with epoxy. This tubing then connected into a rigid conduit that carried the cabling up to the top of the bridge bent. This system was intended as protection against debris and ice floes for the cabling. Black plastic tubing is shown in Figure 2.8 wrapping around the load cell.

The final measure of protection installed was a Lexan polycarbonate shield. The shield was placed on either side of the system to cover the gap between the transducer and bridge column. This was the outermost layer of defense and was intended to deflect larger particles of debris or ice that may have otherwise impacted the more vulnerable parts of the system. The shield was clamped to the system by running threaded rod through from one side to the other and tightening. The side of the shield touching the transducer was tapered and sealed with epoxy to stop debris from wedging between the shield and the loading system. Figure 2.9 shows a photo of the completed protection system at the Big Sioux River site.

Figure 2.10 Installed Monitoring System and Protection

2.2 Laboratory Testing and Validation of the Monitoring System

2.2.1 Laboratory Testing Setup

Laboratory testing was completed for the monitoring system prior to installation. This testing consisted of setting up each system horizontally and loading it at three different locations along the length of the transducer pipe. This simulated different ice impact locations that may occur during data collection. The transducer pipe, load cells, and transducer clamps were assembled identically to the on-site arrangement. The load cells were connected to the laboratory strong floor through a base beam. Figure 2.10 shows a typical test setup.

The same cables used for field installation were used during the test to eliminate influence of wiring. Figure 2.11 shows that the cables and strain gages were marked so they could be installed on site the same way they were installed in the laboratory.

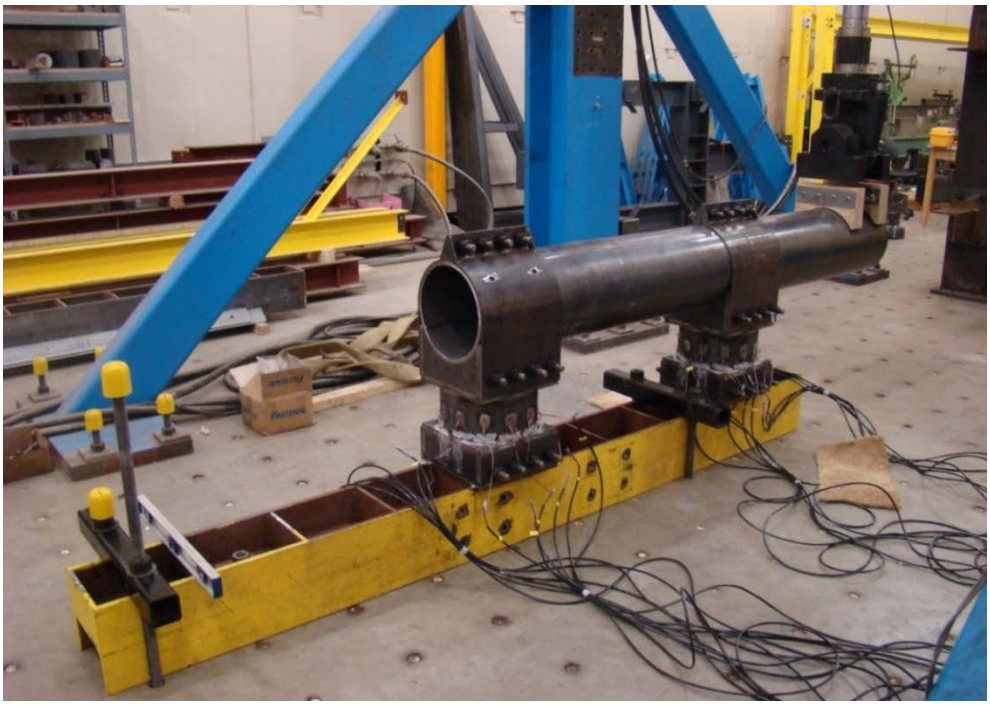

Figure 2.11 Typical Test Set Up for the Monitoring System

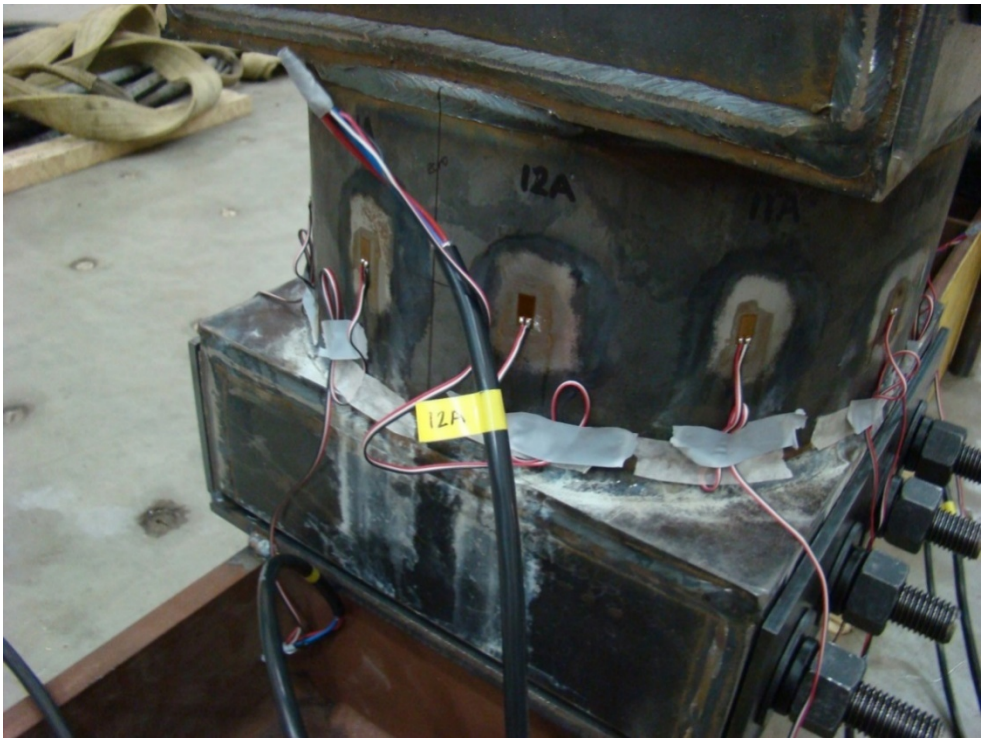

Figure 2.12 Strain Gauges and Connecting Wires

As shown in Figure 2.12, three different loading locations were used in the tests. A 146-kip hydraulic actuator was used to load the system. Each test was run by incrementally increasing the load to 50,000 pounds (50 kips) using the actuator. The laboratory data acquisition system was used to record the load and strain values for each test.

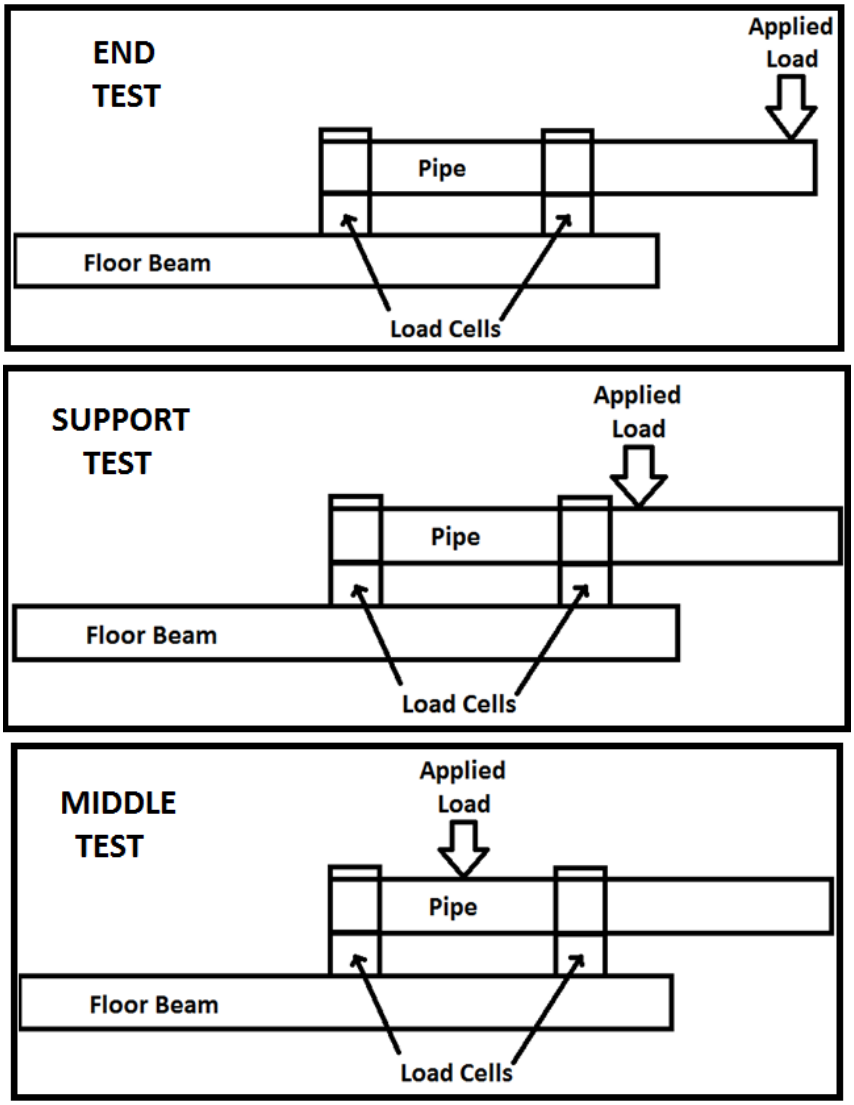

Figure 2.13 Loading Test Configurations

2.2.2 System Accuracy Validation

The strain and actuator load data were recorded for each test. After testing was complete, data were analyzed to determine accuracy of the measurement system by comparing the actual load measured from the actuator load cell to the calculated value based on the strain measurements. First, the strain data from gages on each load cell were averaged. Then the averaged strain was multiplied by the elastic modulus of the steel (29,000 ksi) to get the average stress. This averaged stress was multiplied by the cross-sectional area of the load cell tube (9.16 in^2) to get averaged force. This was done for each load cell. Forces were then added to calculate the total applied load, based on simple force equilibrium. In this process, the strain values indicated either compression or tension on the load cell, with their signs included in the

calculation. This process was conducted for each load step. A linear relationship was achieved between the applied and calculated forces, as shown in Figure 2.13. The comparison of the two forces showed a good fit and the system was determined to have adequate accuracy.

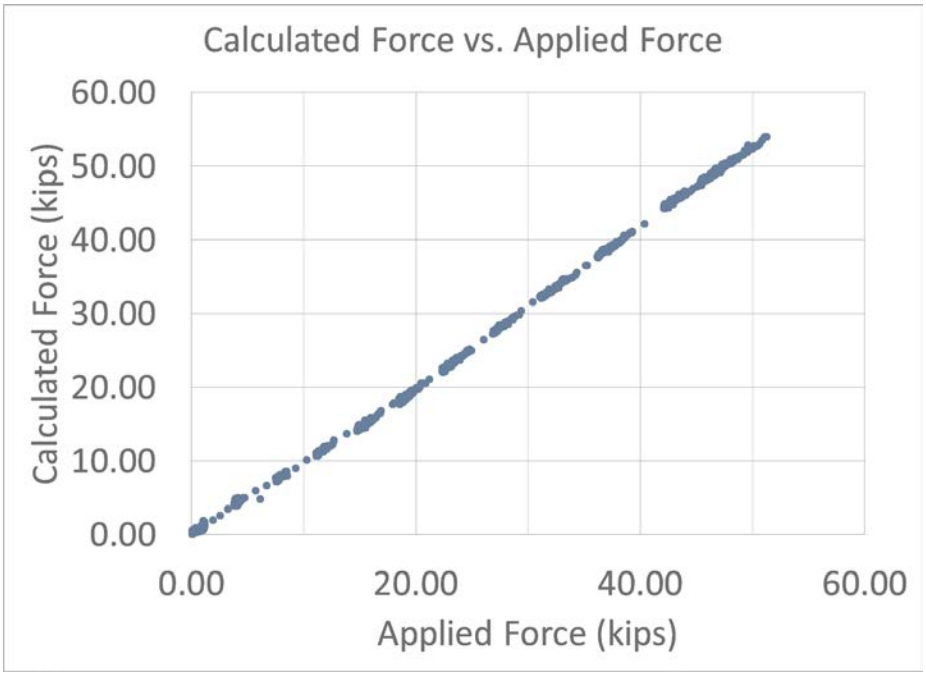

Figure 2.14 Plot of Calculated Force vs. Applied Force

3. MONITORING SITES AND DATA COLLECTION

3.1 Site Selection

3.1.1 Site Selection Considerations

Site selection was critical to achieving this project's objective. Site selection depended on many factors, including measured ice strength and thickness from the previous study, water level change during spring thaw, and feasibility of installation. The starting point for this research was the USGS study which measured ice thicknesses and strengths at several locations across the state from 1999 to 2001. These sites were considered as possible locations for this project because of the data that had been collected. Another resource used to determine locations for installation was the USGS website that contains historical water data across the state. The sites with relatively large ice thickness and high strength were prioritized for selection. In addition, it was desired to choose sites at which a USGS gage was located nearby for water surface elevation data. This data would benefit the project by allowing researchers to position the data acquisition system at an appropriate elevation to collect the data. The possibility of drastic water level changes and ice jams also were important considerations. It would be difficult to design a system to cover a wide range of impact points on the bridge substructure. Also, the possibility of ice jams could increase the likelihood of damage to the monitoring system and would require an extensive protection system.

Bridge ownership was considered in the site selection for practical feasibility purposes. A few county bridges came into consideration from the USGS database; however, it was determined that it would be less complicated to use a state-owned bridge for the purpose of approvals. Another issue discussed was flow path of the river upstream of the bridges. Several sites had flow paths that were complex and would bring in ice chunks from all directions to impact the bridges. This situation would require a more complex system design than what was planned for this project. It may be beneficial to collect data at some of these more complex sites in the future for a thorough consideration of the conditions across the state. For this initial project, however, sites were selected that had straight upstream approaches. This allowed the use of a simple and less expensive design for the monitoring system. Other considerations included ease of access to the bridge piers for installation and shape of the column. The final consideration for site selection process was distance and travel time for the researchers. A site closer to the researchers would allow for quick response time in the event that the system malfunctions. Based on these considerations, two sites were selected for instrumentation—one on US14 over the James River near Huron, South Dakota, and the other over the Big Sioux River on Interstate 29 south of Brookings, South Dakota. Details of the two sites are presented below.

3.1.2 Site 1: James River at Huron

The first site selected was the US14 bridge over the James River just east of Huron, South Dakota. This was one of the sites used in the SDDOT/USGS study discussed previously. Therefore, some historical ice thickness and strength data had been collected for this site. In the USGS study by Niehus, the James River site recorded the thickest and highest strength ice measurements. This site also had water elevation data on the USGS website and a straight upstream approach. The water was relatively deep, so installation required a boat for access to the column. Fortunately, there was a wide ditch along the road that allowed easy approach with no fencing or other obstacles. The bridge was built in 1959 and the bents were oriented parallel to flow of the river, even though this meant that they were not perpendicular to the bridge deck. This is shown in Figure 3.1 below. The bridge is 326 feet and 6 inches in length and 64 feet and 4 inches in width.

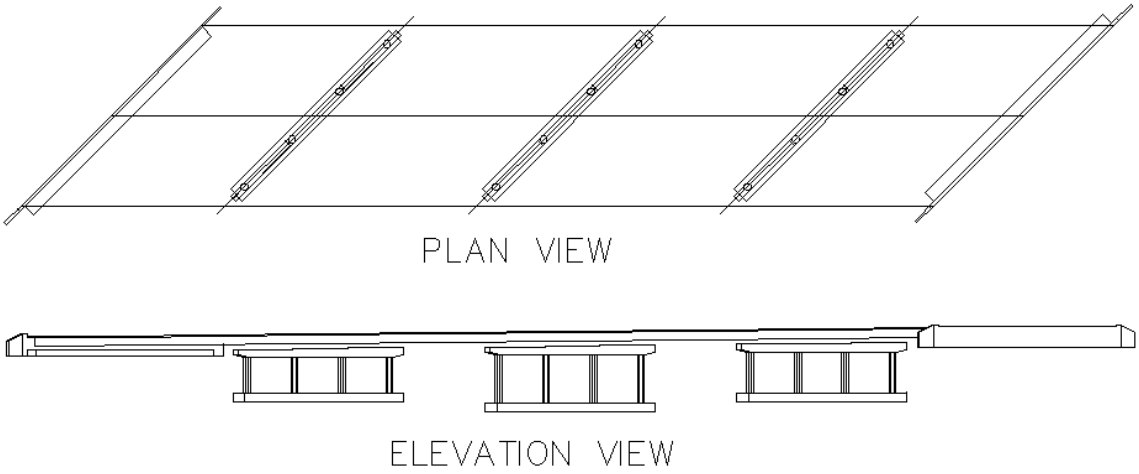

Figure 3.15 Plan and Elevation Views of US14 Bridge over James River near Huron, SD

The columns are 2.5-feet wide and octagonally shaped with shear walls connecting them to one another along each bent. The shape and shear wall design created a challenge in the design of the connection system at this site. Figure 3.2 shows an aerial view of the James River bridge from Google Maps and Figure 3.3 shows a picture taken at the site the winter prior to installation.

Figure 3.16 Aerial View of US14 Bridge over James River near Huron, SD

Figure 3.17 Picture of US14 Bridge over James River near Huron, SD

3.1.3 Site 2: Big Sioux River at I-29

The other site selected was the Interstate 29 southbound bridge over the Big Sioux River located south of Brookings, South Dakota. This site was selected for the simple layout of the bridge, relatively straight approach, availability of water-elevation data, and proximity to South Dakota State University. Access to this site was slightly more challenging, since it is less desirable to close down a lane of traffic on the Interstate. Advantageously a side access road and parking lot typically used in conjunction with a game production area provided access to the site.

The plan and elevation views of the bridge in Figure 3.4 below show that the layout of this bridge is relatively simple. The columns are circular, requiring a relatively simple design of the pier connections needed for this site. This southbound bridge is 400 feet long and 34 feet and 4 inches wide. Figure 3.5 shows an aerial view of the bridge site from Google Maps.

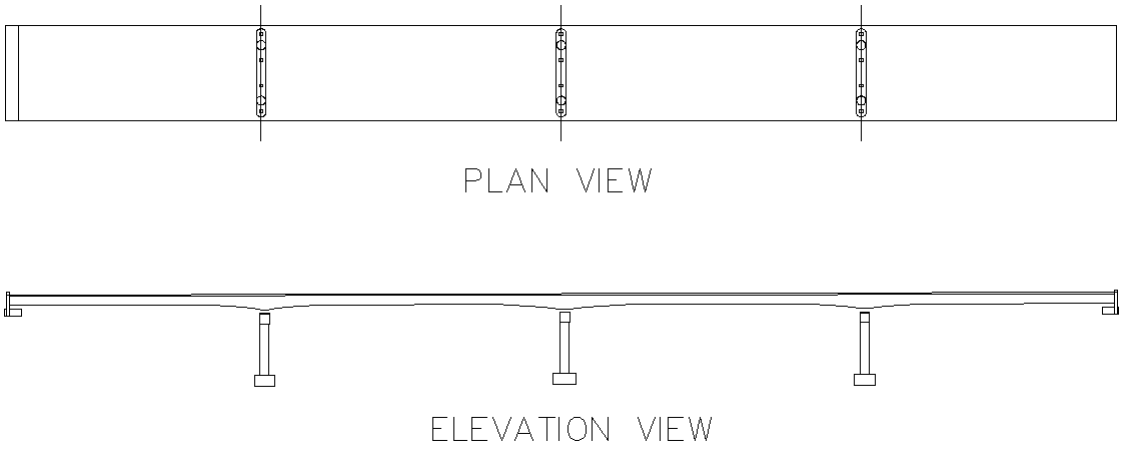

Figure 3.18 Plan and Elevation Views of Southbound I-29 Bridge over the Big Sioux River

Figure 3.19 Aerial View of Southbound I-29 Bridge over the Big Sioux River

3.2 Installation at Monitoring Sites

3.2.1 I-29 Site Installation

Instrumentation at the I-29 site was performed October 10 and 11, 2012. Installation at the site, located south of Brookings on the southbound Interstate 29 bridge over the Big Sioux River, presented a number of challenges. Access to this site was difficult. An access road and parking lot typically used for access to a game production area were used during installation. The parking area was located northwest of the bridge, requiring that all equipment had to be carried across the north fork of the river to gain access to the pier, located in the south fork, on which the instrumentation was installed. Figure 3.6 shows an aerial image of the bridge with the instrumented pier and the access road and parking lot marked.

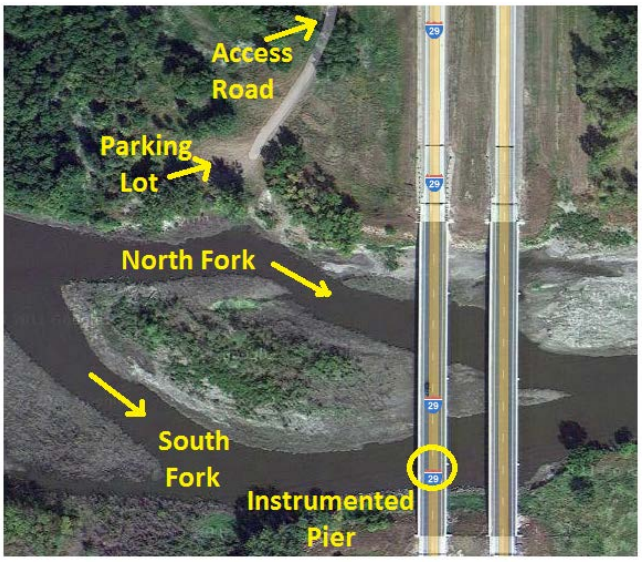

Figure 3.20 Big Sioux River Installation Location

The first step of installation was to mark the location of the transducer system on the column. This location was determined using historical water level data obtained from the USGS website. The pipe was positioned so the lowest water level was not below the transducer pipe and the highest was not above it. However, due to wide variability of water levels at the site and length limitation of the transducer, the 5-year maximum water table exceeded the top of the transducer. The transducer was protected to be water resistant. Thus if the 5-year maximum event happens, part of the ice float data will not be collected. Due to the broad flood plain at this location and the low likelihood of this maximum event, the water had never topped the pier during the entire study period. Figure 3.7 shows the historical water levels relative to the proposed installation location.

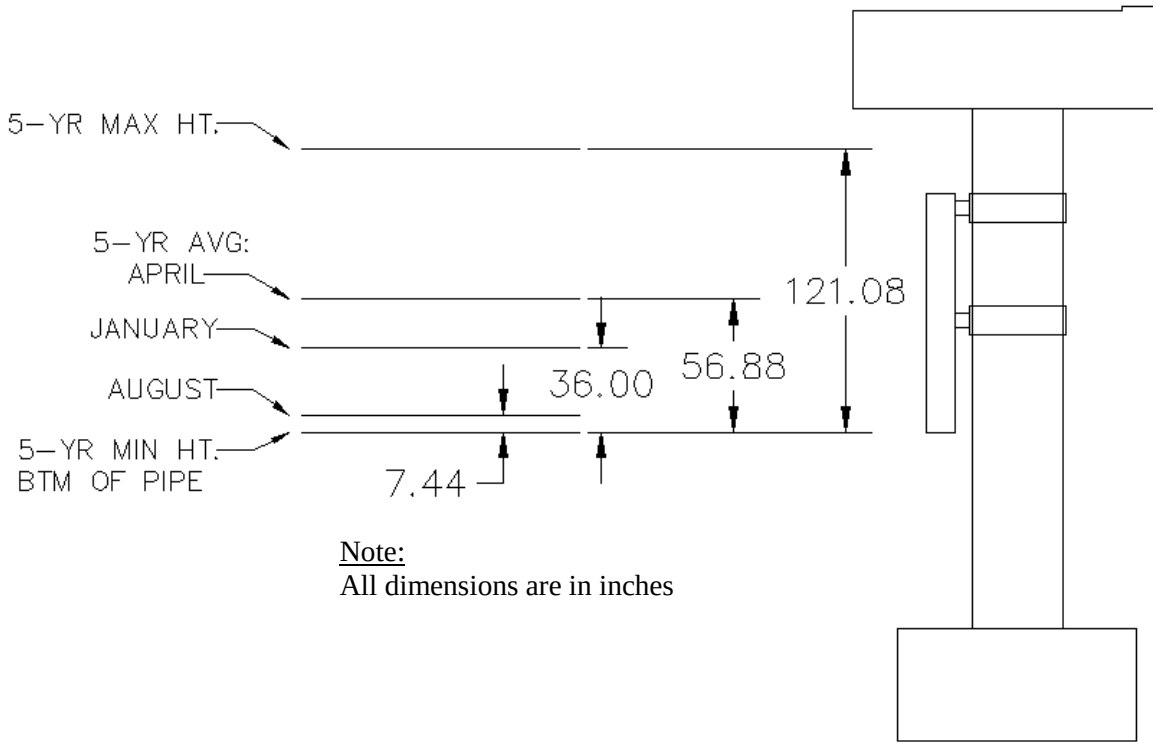

Figure 3.21 Big Sioux River Historical Water Elevations

Once the location was marked, installation of the load cells commenced. The relatively low water levels at this site allowed workers to access the bridge column using waders. Two levels of scaffolding were erected on both sides of the column to assist in reaching necessary heights on the column to install load cells. A beam was positioned atop the bent cap so the ends extended out on either side. Pulley systems were attached to this beam for assistance with lifting the components of the system. Figure 3.8 shows the pier with scaffolding and the beam and pulley system during installation.

Load cells were lifted and held in place using the beam and pulley system while the clamps were placed. After both load cells and clamps had been placed, holes were drilled for the anchors. Holes were drilled at locations where there was no column reinforcement (approximate depth of the holes was less than 2 inches). Extra care was taken during installation to avoid damaging column structure and reinforcement bars. Epoxy was injected into the holes using an injection gun, and then ½" diameter threaded studs were inserted into the epoxied hole. Anchors were placed around the column through the clamps to resist torsional forces applied to the system. After the epoxy cured, the bottoms of the clamps were sealed and the 0.5-inch gap left by the spacing rods was filled with non-shrink grout. The grout was used as a secondary means of attachment and extra friction for the clamps to connect with the column.

After the load cells and clamps were secured, the transducer pipe was transported from the parking lot to the pier using a small boat. The pipe was then lifted into place using the pulley system. Once positioned, the pipe was secured to the load cells using the outside clamps.

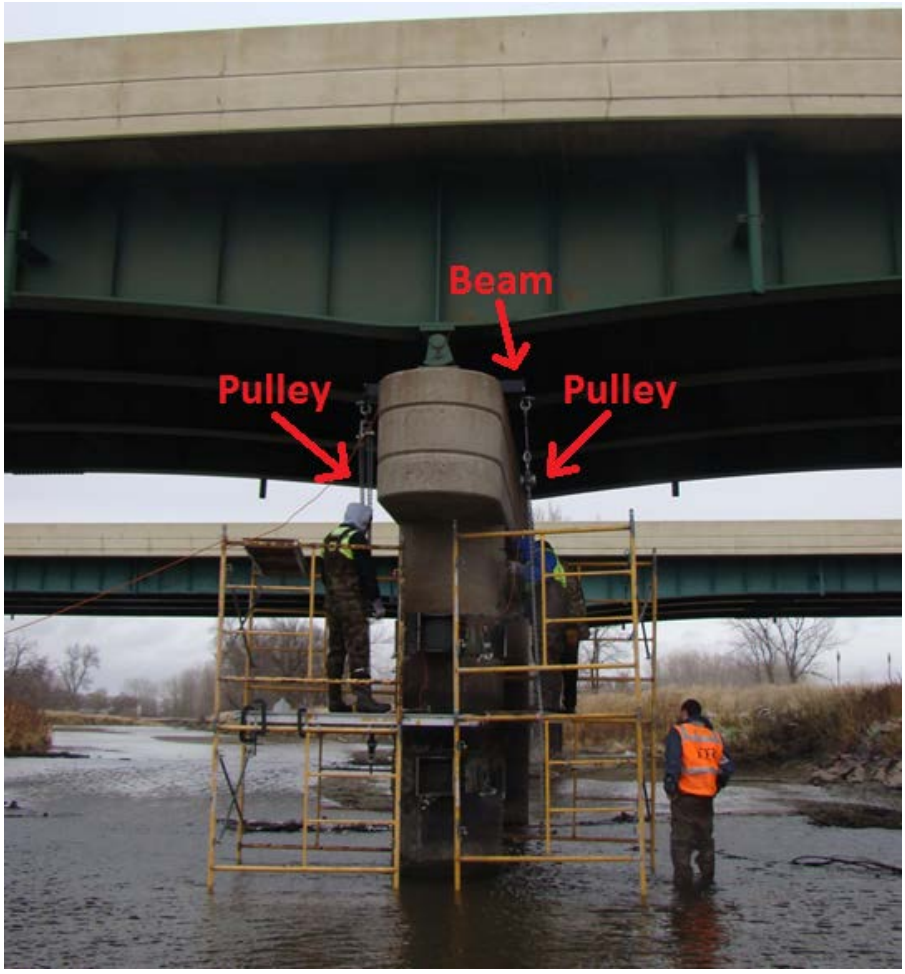

Figure 3.22 System Installation at Big Sioux River Site

Following installation of the mechanical system, the cables (approximately 130 feet long) were threaded through girders on the underside of the bridge deck from the southern abutment to the pier. This could not be done from the ground; therefore, a bridge inspection unit (commonly referred to as a snooper) was provided and operated by the S.D. Department of Transportation. The snooper is a truck with a telescoping hydraulic boom and basket that enables up to three people to move around under the deck of a bridge. Figure 3.9 shows a photograph of the snooper being used during installation.

Figure 3.23 SDDOT's Snooper Truck

The outside lane of southbound traffic was closed during this part of the installation process. Cables were pulled through the rigid conduit installed on the pier by a licensed electrician. Cables were attached to the gage wires and protected in the black tubing as previously shown. This tubing was filled with epoxy to fully protect connections from water damage. Lexan polycarbonate sheets were then placed on either side of the pipe and secured using the threaded rods. The edge of the sheets located on the transducer pipe was sealed using epoxy to protect from debris wedging inside the polycarbonate sheets.

Along the underside of the bridge deck, the cables were attached using rigid conduit straps that had been wrapped with electrical tape and rubber padding. Straps were secured to the bridge deck using concrete screws and were spaced every 6 to 10 feet from the pier to the abutment. Access was provided by the snooper. The data logger was installed in the weatherproof box along with the battery, cell modem, and photovoltaic controller prior to reaching the site. The box was then attached to the south abutment of the bridge underneath the deck as shown in Figure 3.10.

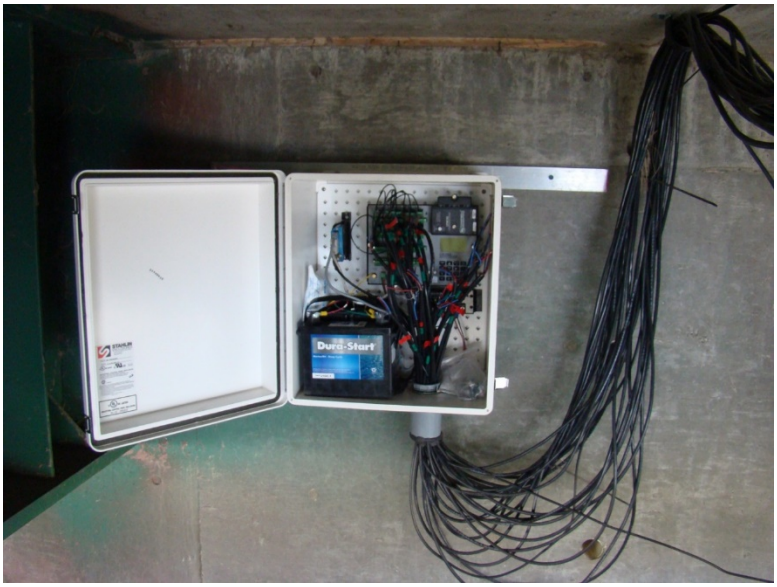

Figure 3.24 Installed Weatherproof Box for the Data Logger

The cables that attached to the strain gages on one end were connected to the data logger on the other end using quarter bridge connection. The solar panel was mounted on a Telspar sign post approximately 30 feet from the end of the bridge in the road ditch. The power cable ran through partially buried conduit from the solar panel to the photovoltaic controller, which was located in the weatherproof box under the bridge. Finally, an antenna was attached to the side of the bridge and connected to the cell modem.

3.2.2 US14 Site Installation

Instrumentation at the US14 site was performed October 2 and 3, 2012. Installation at the site, located east of Huron on the US14 Bridge over the James River, was similar to the I-29 site in many ways, but provided its own set of challenges. The average daily traffic at this site was also less at this site, resulting in less congestion. The ditch near the bridge was wide and shallow enough to drive vehicles down for easy access to the bank of the river. The main installation challenge faced at this site was the five-foot depth of the river near the pier. Therefore, all work on the column had to be completed from either the snooper or the boat, shown in Figure 3.11, that was provided by the Department of Game, Fish, and Parks.

Figure 3.25 Monitoring System Parts at James River Site

As at the other site, the first step in the installation process was to locate ideal positioning of the monitoring system on the column using information obtained from the USGS website. Figure 3.12 shows the pier relative to the 5-year historical water levels.

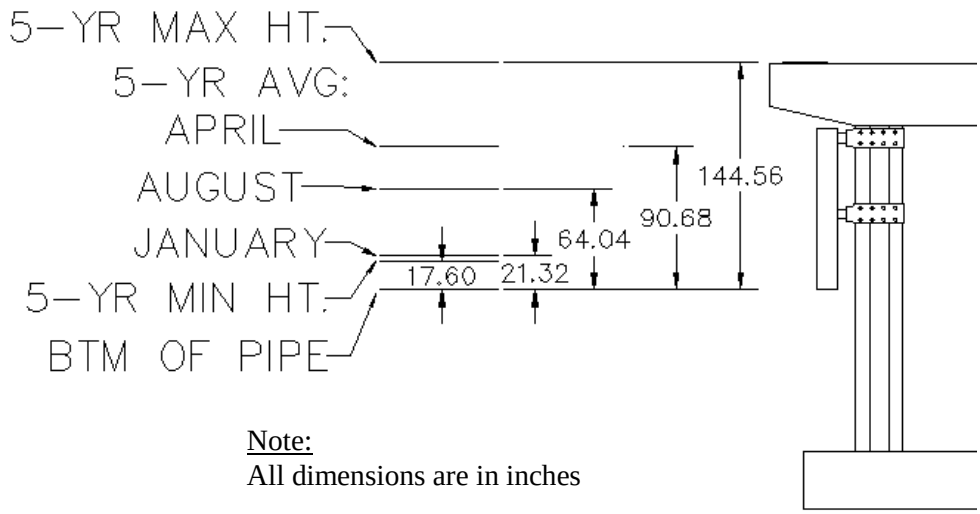

Figure 3.26 James River Historical Water Elevations

Once the location was marked, the beam and pulleys were positioned across the top of the bent cap to assist in lifting and holding pieces in place during installation. The cuffs were the first pieces moved into position. They were held by the pulley system, and marks were made where the anchors would be placed. Once the anchor locations were marked, the cuffs were moved and the holes were drilled with caution to avoid existing steel bars in the sub-structure. The drilling depth was limited to approximately less than 2

inches. After holes had been drilled, cuffs were repositioned and anchors were installed using epoxy and 5/8” threaded studs. Figure 3.13 shows workers placing cuffs and anchors on the pier.

Figure 3.27 Installation of the Monitoring System Cuffs and Anchors

Anchors were placed and allowed to cure before the load cells were installed. After curing, load cells were attached and the transducer pipe was lifted out of the boat and swung into position using the pulley system. The pipe was then secured using the clamps as discussed previously. Figure 3.14 shows installation of the pipe.

Figure 3.28 Installation of Transducer Pipe at the James River Site

Next, approximately 150-foot-long cables were run under the bridge deck and pulled through the rigid conduit installed by a licensed electrician on the column. Once the cables had been pulled through the conduit, they were attached to the strain gage wires and protected using epoxy-filled black plastic tubing. The polycarbonate shields were then installed similar to the Big Sioux River installation. Using the snooper, the cables were secured to the underside of the bridge deck with conduit straps that had been wrapped in rubber and electrical tape. These were anchored using concrete screws. The straps were spaced at 6- to 10-foot intervals from the pier to the end of the bridge. Once the cables had reached the end of the bridge they were run through rigid conduit from under the bridge deck to the weatherproof box containing the data logger, battery, cell modem, and photovoltaic controller. The box was mounted on a Telspar sign post with the solar panel and antenna.

3.3 Ice Load Data

In this section, the data collection and analysis procedures are presented. The first sub-section describes the data collection processes. The post-processing procedure is described in the second sub-section. Finally, data resulting from two years of monitoring and the statistical analysis of these data are presented in the third sub-section.

3.3.1 Data Collection Procedure

As discussed previously, 14 channels of data were collected. Twelve channels were strain gages, six on the top load cell and six on the bottom load cell. The other two were thermocouples, one recording the temperature on the top load cell and one on the bottom. The maximum frequency the data logger could support for 14 channels of data collection was 5 hertz (5 data points per channel per second).

The use of a trigger to record data was done only after an event was considered. In the end it was decided to use two 1-GB memory cards and record data at the 5-Hz rate continuously. The data logger itself had a small amount of memory and was capable of storing data during the time it took to switch from one memory card to another. Therefore, two memory cards were used for each data logger. After one memory card had been collecting data for a certain amount of time, researchers would replace the card that contained data with a blank card. Data collected during this transition period was saved to the data logger's internal memory, then transferred to the second memory card once the switch was complete. The memory cards had the capacity to record data over all channels at the rate of 5 Hz for a span of 90 days. During the collection period, the memory cards were swapped about every two weeks to minimize the potential loss of data and to maintain a visual log of the conditions on site. After all of the data had been collected, the strain values were converted to force in each load cell. Using force equilibrium introduced earlier, the total force applied to the system was then calculated.

3.3.2 Post-Processing

The first step of post-processing was condensing data to a manageable size. The amount of data collected was much more than necessary for the purpose of identifying maximum ice forces. Thus condensed data points were taken at every fifth recording step from the raw data, making the effective data sampling rate 1.0 Hz. Data collected before ice formed in the waterway and after complete melt of ice at each site were also discarded based on estimated dates. For both sites, winter seasons included in the data collection were 12-21-2012 to 4-16-2013 and 12-2-2013 to 4-4-2014. Figure 3.15 and Figure 3.16 illustrate the converted force and temperature (average temperature of two load cells) data collected during the two years.

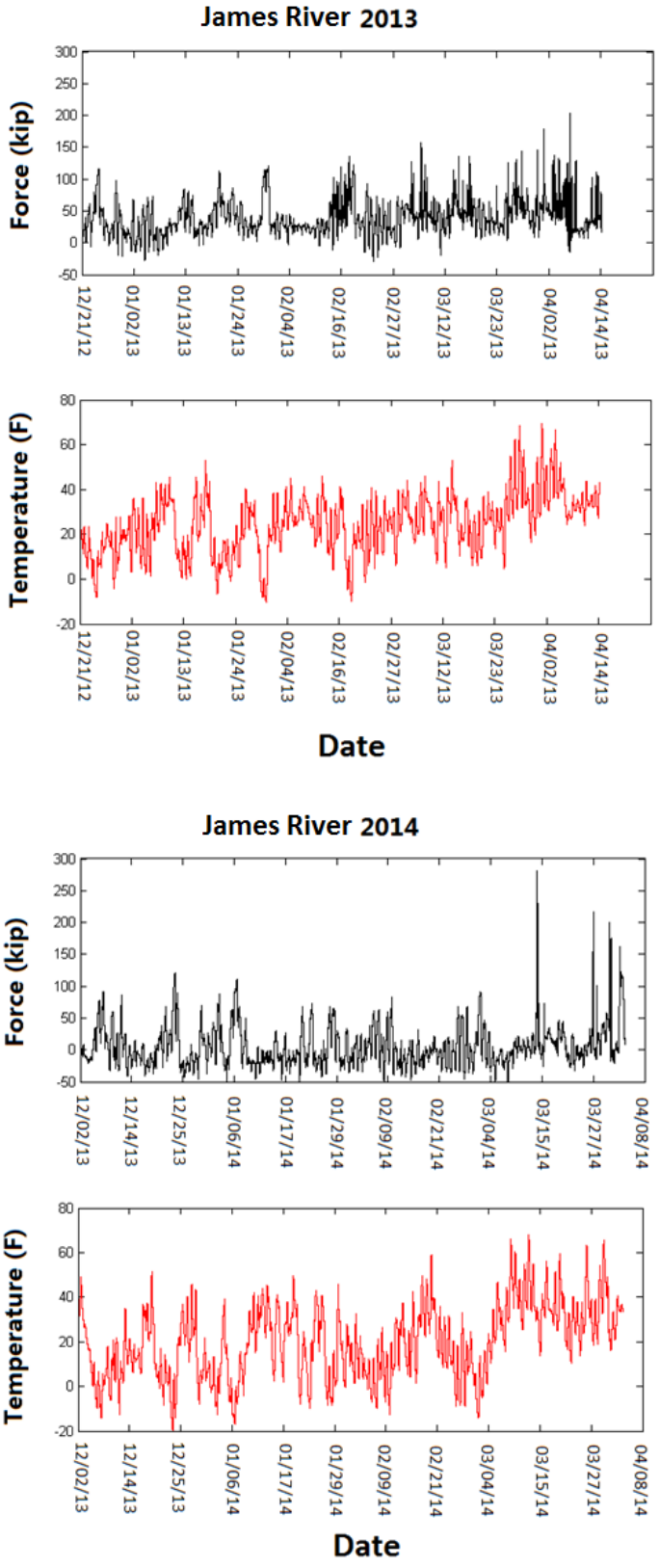

Figure 3.29 Unprocessed Data at US14 James River Site

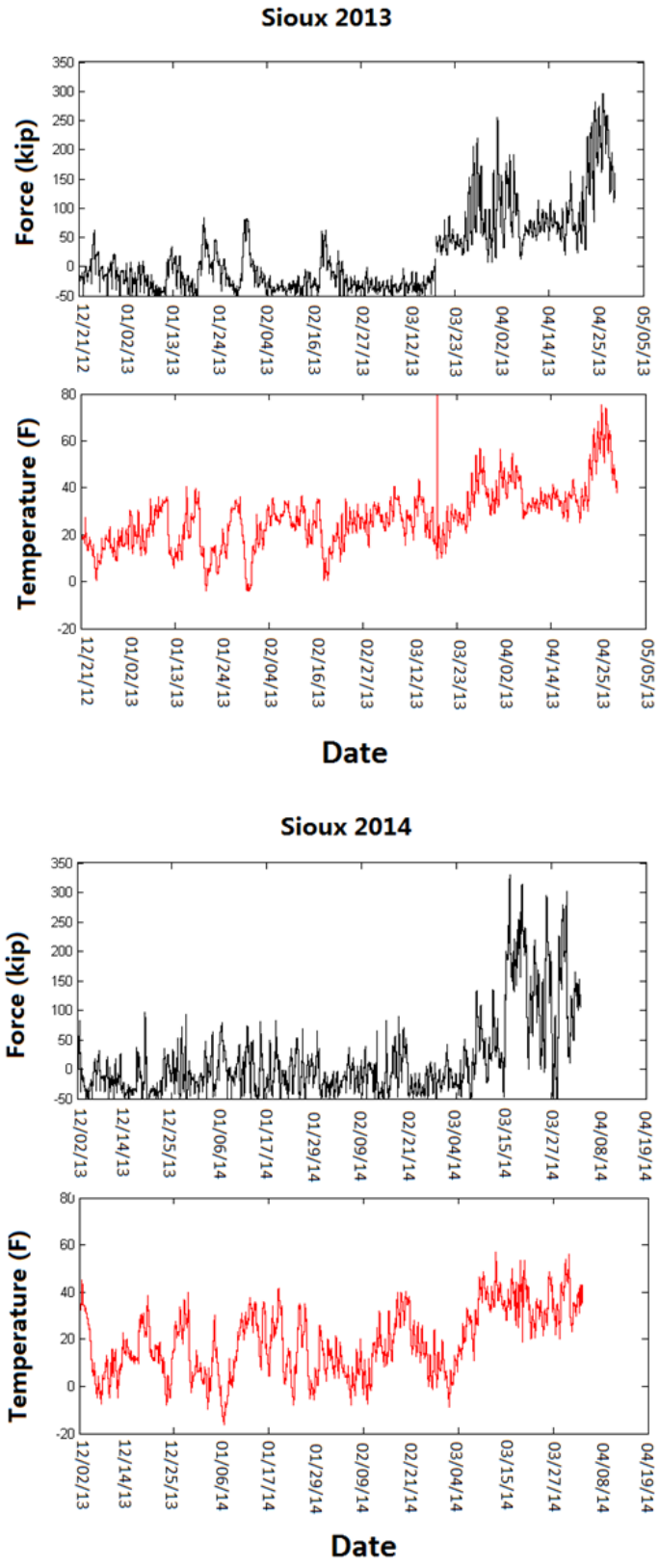

Figure 3.30 Unprocessed Data at I-29 Big Sioux River Site

The above figures clearly show a similarity between overall fluctuation of force measurements and temperature measurements. Either there was a direct relationship between ambient temperature and ice load all the time, which is not logical, or the strain measured by the load cell was affected by temperature. Some spikes of temperature measurement were observed, but were likely caused by error in instrumentation. An examination of the temperature and calculated force from strain data for about 18 days demonstrates a clear pattern of daily fluctuation on both sites (Figure 3.17). The ice load value calculated directly from the raw data was not likely the real ice impact load. Thus, the long term trends in the strain gage measurement do not necessarily represent real increase in loads.

The reason for this fluctuation may have been temperature sensitivity of the strain gauge and steel material. Although impact of temperature on the strain measurement can be eliminated using the measured temperature data (through thermocouples attached at each of the load cell), this compensation will not yield accurate results if the structure is not allowed to expand and contract freely under temperature variations. Although the idealized force transfer is a simply supported HSS pipe with overhang, the actual installed structure is an indeterminate system in which temperature-induced strain variation is different from that in determinate structures. Without precise knowledge on the nature of the actual boundary conditions for the installed system, it is difficult to identify and compensate for the temperature-induced strain fluctuation, but any temperature-induced measurement will trend with the temperature fluctuation and can be removed from the data by using a highpass filter, because temperature will not vary rapidly). As shown in Figure 3.17, where both the force measurement and temperature measurement were normalized and plotted to overlap each other, some short period ice load surges can be observed “riding” on temperature-induced fluctuation. These high-frequency fluctuations are believed to represent the true impact ice loads experienced by the monitoring devices.

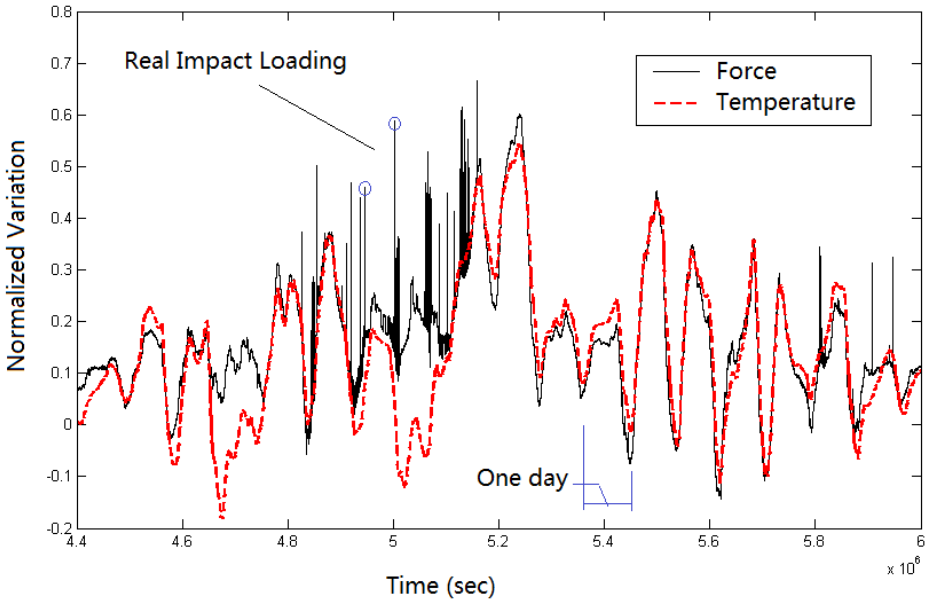

Figure 3.31 Example of Impact Load Data Riding on Temperature-Induced Fluctuation

The built-in Matlab Butterworth filter (a 4^{th} order highpass filter that filtered out frequencies lower than 5.56×10^{-4} Hz (period longer than 30 minutes)) was used to filter out any fluctuation with a period longer than 30 minutes from the data. After the filtering operation, a zero baseline was created with the short-term spikes riding on it. Due to characteristics of the filtering process, the filtered signal also included some negative peaks. The negative peaks typically appear right after a positive peak due to the shape of the sudden spike in a relatively smooth time history. However, as these peaks still represent a sudden change in the data that may relate to impact loading, the magnitude (absolute value) of these peaks also included in the estimate of the impact loads. Therefore, the estimation of the peak ice load is conservative. Figure 3.18 shows the plot of force vs. time, after the filter was applied, for both sites over the two-year period. Most of the impact events happened during the spring thaw period.

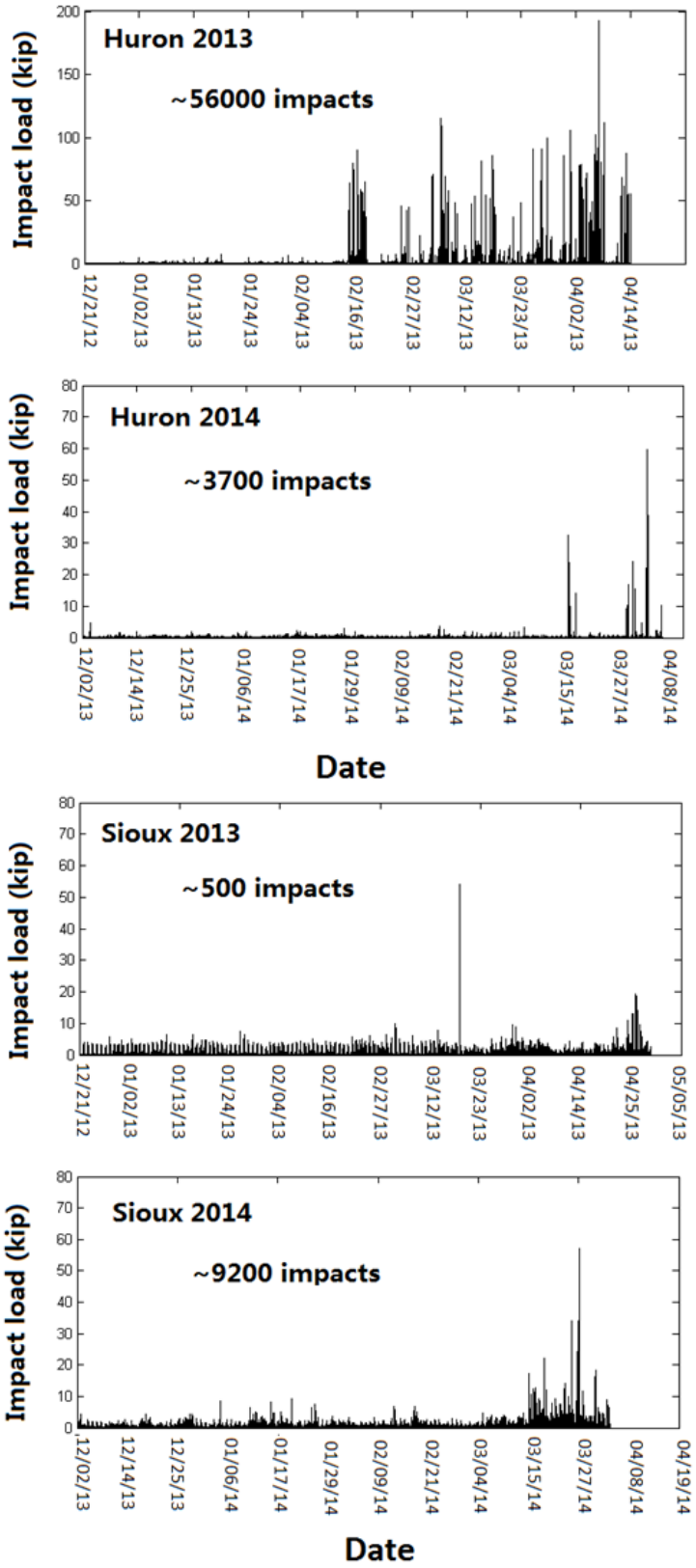

Figure 3.32 Filtered Ice Impact Force Data

Once all data had been filtered, a program was developed in Matlab to investigate positive peaks, which represent the maximum impact ice loads measured during the monitoring period. Only forces greater than 10 kips were considered in the analysis, as the sensitivity of the monitoring device to smaller load levels may be questionable. If we consider ice impact load as a random variable, the histogram of the impact load can be plotted as in Figure 3.19 and Figure 3.20. A histogram was generated with all of the data from the two-year period at each site.

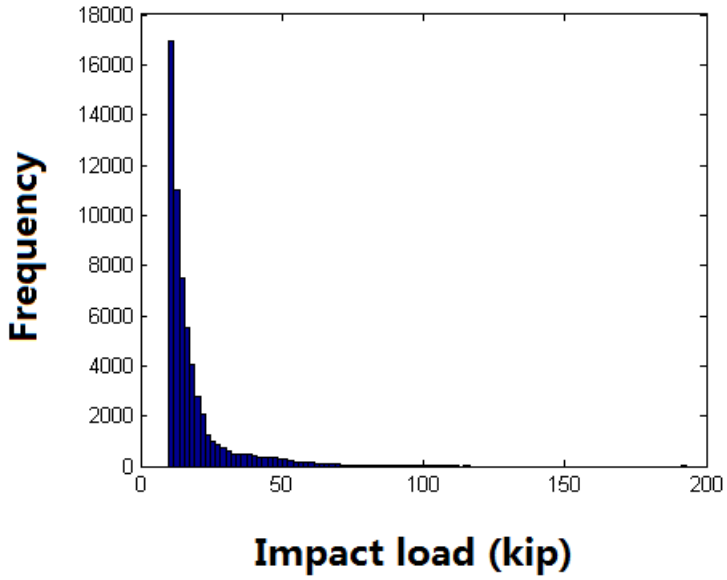

Figure 3.33 Histogram of the Individual Ice Impact Load at James River Site

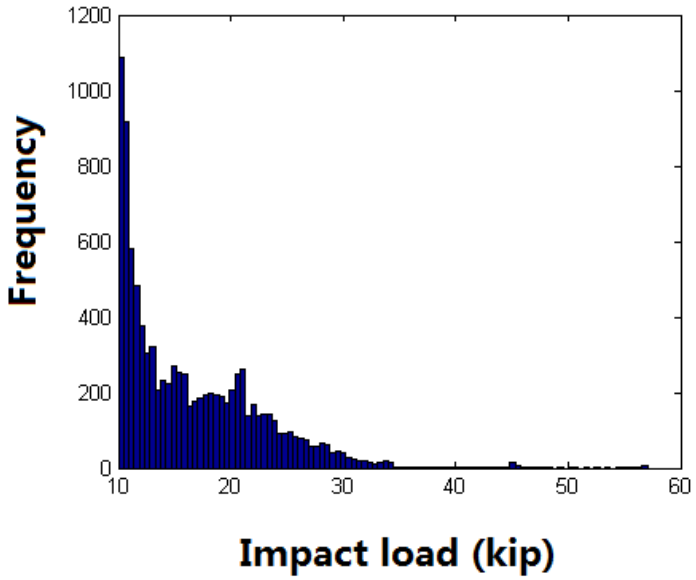

Figure 3.34 Histogram of the Individual Ice Impact Load at Big Sioux River Site

Statistical analysis reveals more insights from the data. The first question may be whether there is any difference in data between different sites and different years. It is logical that these data are different, as the topology and hydraulics at the two selected sites are quite different and the two consecutive winters (2013 and 2014) were not exactly the same. In fact, the hypothesis tests (t-test) of the four groups of data

confirmed this suspicion. The standard t-test, which is routinely used to judge if the means of two different sample groups are the same, was used here to compare the mean value of these subsets of the data. At the 0.05 significance level, the James River ice load was significantly different from the Big Sioux River ice load when all data from both years are considered. At the James River site alone, the 2013 data at the site was statistically similar to the 2014 data. However, for the Big Sioux River site, the data from the two different years were statistically different. This comparison suggests that variability of the ice load depended on location and weather. As a first attempt to gather realistic ice load data, duration and scope of this project was relatively limited for the purpose of capturing the average trends of extreme ice load in South Dakota rivers. Gathering data at more locations over a longer period of time will be beneficial for developing a more comprehensive understanding of river ice loads.

Since it was expected that the ice load statistical distribution at each site would be different, as confirmed by the statistical testing, it was logical to develop an extreme ice load model based on data from each site. Several extreme distribution models were used to fit the peak ice load data over two years of data collection at individual sites. As shown in Figure 3.21, the lognormal model was a reasonable fit for the tail of the ice load distribution. It was adopted in this study to extrapolate extreme ice load events for the design life of the structure. The fitted parameters for the lognormal distribution representing single impact events are shown in Figure 3.21. These fitted parameters (mu and sigma shown in Fig. 7-21) are the result of least-square regression, representing the lognormal distribution parameters that best represents the observed ice impact data. They will be used later in the reliability calculation to estimate maximum ice impact load in a longer design life span.

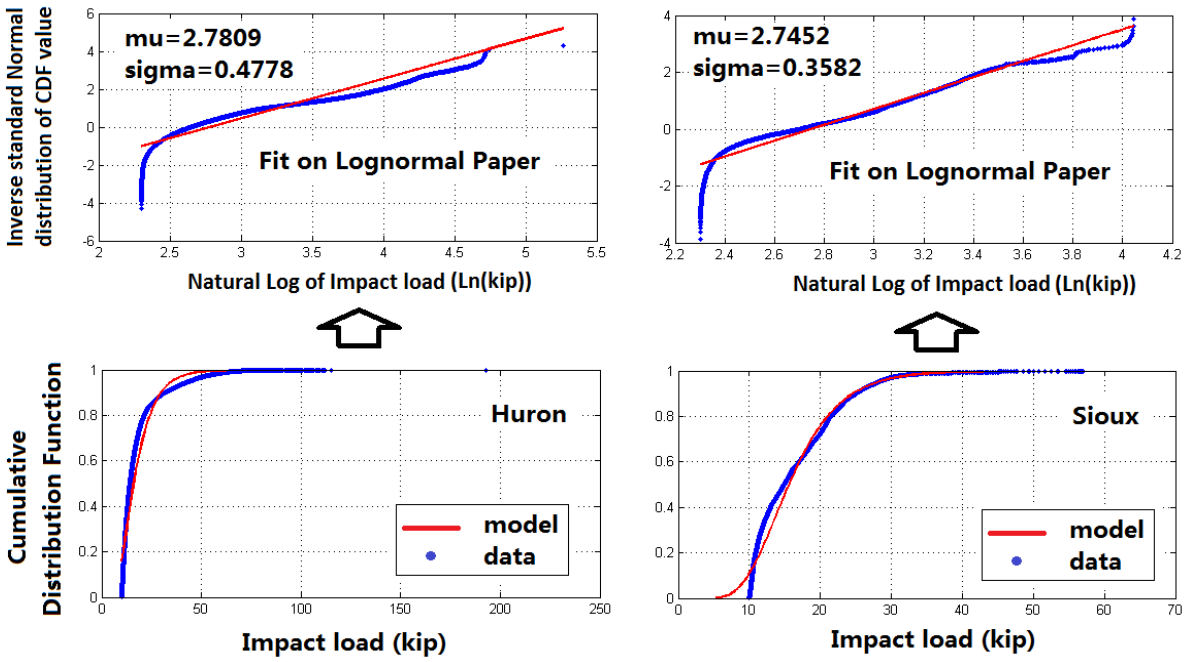

Figure 3.35 Lognormal Model Fitting for Impact Load Data Greater than 10 kips

3.4 Additional Ice Strength Measurements

At the beginning of the project, it was deemed helpful to collect mechanical properties of ice that formed during the ice load data collection period. In this study, ice thickness and compressive strength were obtained during winter periods at both sites. However, it was later discovered that it is inaccurate to use ice strength measured at a particular time during the winter (when the waterway was completely frozen)

as an indicator of impact ice strength at spring thaw. During spring thaw, the ice float can be tested for strength. However, due to the increase in ambient temperature and water content in ice cores, the ice core will be very “ductile” and the strength at which the ice will fail in compression cannot be identified. The research team visited both monitoring sites several times during the monitoring period and conducted multiple tests using the equipment shown in Figure 3.22. Figure 3.23 shows on-site ice sampling at the James River site during the 2013 winter season.

Figure 3.36 Equipment for Ice Coring and Measurement of Ice Strength

Figure 3.37 Researchers Taking Ice Core Samples at the James River Site

The ice compressive strength was measured by conducting compressive strength tests on cylindrical ice samples. The samples were obtained by drilling ice cores of approximately four inches in diameter. The cores were then sawed off at the ends to create even surfaces for uniform loading. Each ice cylinder was tested in compression to failure (cracking and splitting of the cylinder, signified by a sudden drop in the load-ring reading). Figure 3.24 shows a test sample placed in the compression testing apparatus. The maximum load read from the load ring was recorded as the failure load. Compressive strength of the ice

specimen was calculated by dividing failure load by the cross sectional area of the sample. Even for a single core, there were differences between strength of ice near the top of the surface and strength near the bottom of the ice layer.

Figure 3.38 Compressive Strength Test Setup of an Ice Core Sample

The ice strength measurement was not found to correlate with measured ice loads. This was expected because ice impacting the bridge during spring thaw does not have the same strength as measured during middle of the winter. Ice samples collected close to spring became ductile and did not have a clearly identifiable strength. The data obtained from this study are listed in the Table 3.1 and Table 3.2 for reference purposes.

Table 3.2 Measured Ice Crushing Strength at the James River Site

Sample #	Diameter (in)	Length (in)	Failure Load (lb)	Strength (psi)
2/28/2013, James River, thickness 17"				
1	3.88	7.75	4850	406
2	3.88	7.23	3888	319
3	3.92	8.94	6026	489
4	3.76	5.25	4267	391
5	3.86	6.75	4327	366
6	3.98	5.88	5033	413
3/14/2013, James River, thickness 16"				
1	4.00	7.06	3204	255
2	4.00	6.50	2671	213
3	3.87	7.00	3310	281
4	3.87	5.63	4007	340
5	4.00	5.00	2973	237
6	4.00	8.00	3127	249
2/20/2014, James River, thickness 12"				
1	4.00	4.50	4457	355
2	4.00	3.25	6595	525
3	4.00	3.50	2016	160
4	4.00	3.00	1560	124
5	4.00	5.50	5995	477
6	4.00	4.50	5368	427
3/6/2014, James River, thickness 18"				
1	4.00	5.00	3291	262
2	4.00	5.25	3223	257
3	4.00	6.00	2772	221
4	4.00	7.00	4357	347

Table 3.3 Measured Ice Crushing Strength at the Big Sioux River Site

Sample #	Diameter (in)	Length (in)	Force (Ib)	Strength (psi)
3/14/2013, Big Sioux, thickness N/A				
1	3.87	7.25	1904	161
2	3.87	6.50	2118	180
3	4.00	5.12	2836	226
2/20/2014, Big Sioux, thickness 9"				
1	4.00	6.00	7743	616
2	4.00	3.75	4833	385
3	4.00	4.00	7153	569
4	4.00	6.25	4580	364
5	4.00	7.50	4307	343
6	4.00	7.25	4670	372
7	4.00	7.50	2474	197
3/6/2014, Big Sioux, thickness 16"				
1	4.00	7.00	3417	272
2	4.00	5.75	3642	290
3	4.00	7.75	2781	221
4	4.00	7.75	3349	267
5	4.00	6.25	3368	268

4. RELIABILITY EVALUATION

In this section, distribution of the extreme ice load value derived in the previous section was used to estimate maximum ice load statistics for a given design life. Reliability of the AASHTO empirical equation was evaluated by comparing calculated design load with measured maximum load. Probability of the actual load exceeding the AASHTO design load under different conditions was evaluated.

4.1 Extreme Ice Load Statistics

In the previous section, the ice impact load was modeled as a random variable following a lognormal distribution. Based on distribution of single impact events, distribution of the maximum impact load in any given time span can be derived, if we assume individual events are independent. In addition, it was assumed that the average number of impact events at a given site is constant for each year. Based on impact data gathered at the two sites during this study, it is quite apparent that the number of impacts at a given site can vary from year to year. However, due to limitation of the available data, the average impact count in the two years of monitoring was used as the average annual impact count. In this study, an impact event is defined as any filtered peak exceeding 10 kips. Table 4.1 lists the total number of impact events in the monitoring period at both sites.

Table 4.4 Total Impact Events Greater than 10 kips

	James River	**Big Sioux River**
2013 Winter	56535	509
2014 Winter	3715	9191

As shown, impact numbers for each site is quite different, which can be expected because of differences in geometry of the waterway and flow characteristics. On average, we assumed that the number of annual impact events is 30,000 at the James River site and 4,800 at the Big Sioux River site. Thus the total number of impact events during the design life of a bridge (assuming 75 years) will be 75 x 30,000 = 2,250,000 for the James River bridge and 360,000 for the Big Sioux River bridge. Based on fundamental probability theory, the cumulative distribution function (CDF) of the maximum impact load for these sites can be calculated as shown in Equation 4.1:

$$F_{max}(X) = F_{single}(X)^N \qquad \textbf{Equation 4.3}$$

Where $F_{single}(X)$ is the CDF of an individual event, and $F_{max}(X)$ is the CDF for maximum impact load considering the individual impact event happens *N* times. The underlying assumption is that all impact events are independent and represent samples from the same distribution. Although quite simplified, these assumptions are logical and present a plausible result given the limited information from only two years of data. The distribution of the maximum ice load in 75 years for each site is plotted in Figure 4.1. Using the CDF function given above for the 75-year extreme event, the probability of exceedance at any given load level *X* can be calculated as shown in Equation 4.2:

$$Pr = 1 - F_{max}(X) = 1 - F_{single}(X)^N \qquad \textbf{Equation 4.4}$$

The curves below were generated using Equation 4.1 and Equation 4.2, using the fitted lognormal parameters shown earlier for the single impact event (blue curve). The 75-year maximum event curve (red) was generated using Equation 4.2.

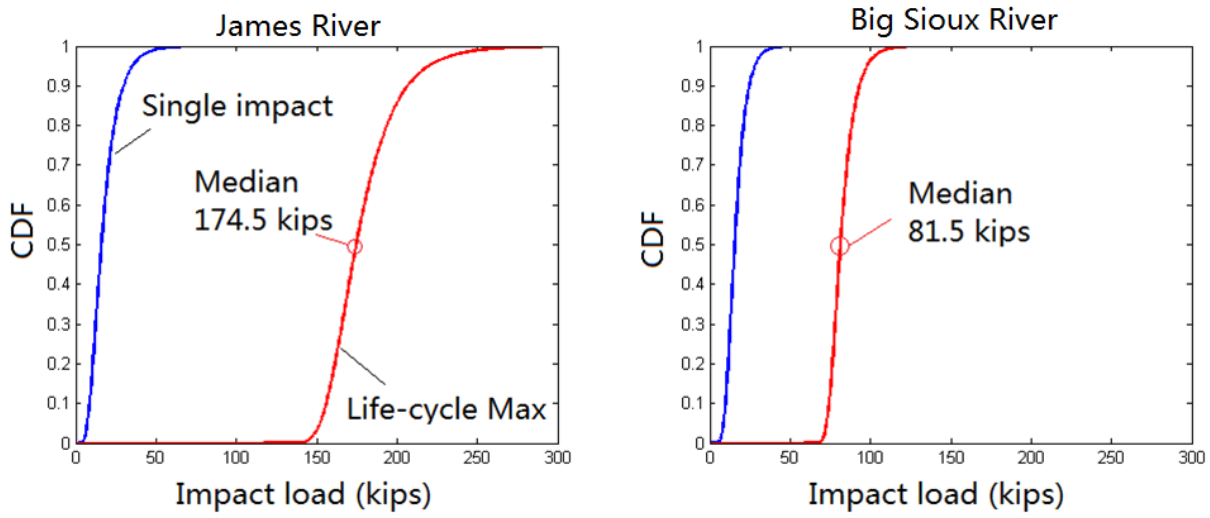

Figure 4.39 Transfer of Individual Impact CDF to 75-year Maximum Impact CDF

4.2 Comparison to AASHTO Ice Load Design Loads

As discussed previously, the S.D. Department of Transportation (SDDOT) currently uses the AASHTO LRFD Bridge Design Specifications (AASHTO 2014) calculations when designing new bridges. The crushing force case controls for the two sites studied since the piers are vertical and the ice will not fail in bending. To compare the forces measured to the AASHTO code, calculations were completed using the transducer pipe as the column (w = 12.75 inches = 1.0625 ft) for both sites. Since a variety of options on effective ice strength are provided by AASHTO depending on the condition of the ice (four levels at 8, 16, 24, and 32 ksf), it is unclear what ice strength level provides a reasonable estimate. Based on the ice-thickness map generated from the previous study, it is reasonable to assume that ice thickness at the monitoring sites could be taken as 2.5 ft. This yields a w/t ratio smaller than 6. Thus the applicable AASHTO ice load formula is as follows:

$$F_c = C_a\, p\, t\, w \qquad \textbf{Equation 4.5}$$

$$C_a = \left(\frac{5\,t}{w} + 1\right)^{0.5} \qquad \textbf{Equation 4.6}$$

In addition, for small streams, the AASHTO code allows a maximum 50% reduction factor (k_1) to be applied to the calculated design load. With the actual A/r^2 value of the two sites unknown, we can assume the maximum reduction in order to explore the bounds for AASHTO design load.

Table 4.5 Design Ice Loads per AASHTO Code

	Design Ice Loads (kips)			
Effective Ice Strength (ksf)	8	16	24	32
James River Site with Reduction Factor	61	122	184	276
James River Site without Reduction Factor	122	245	367	551
Big Sioux River Site with Reduction Factor	37	73	110	147
Big Sioux River Site without Reduction Factor	73	147	220	294

Based on this assumption, the codified ice load for the two monitoring sites on a 1-ft diameter circular column is listed in Table 4.2.

The equation for the reliability index is:

$$P_f = \phi(-\beta) \qquad \textbf{Equation 4.7}$$

Where:

P_f = probability of failure
$\phi(x)$ = standard normal cumulative distribution function
β = reliability index

Based on the definition, a reliability index of 3.5 is equivalent to a probability of failure of 2.3×10^{-4} (approximately 1 in 4350) during the 75-year design life of a structure. However, this probability of failure is calculated considering both probabilistic distribution of the demand, structural capacity, and the design approach itself. In this study, the only information we have is on the load side. Thus we can only investigate probability of the actual maximum ice load in 75 years exceeding the codified ice load calculation results under different conditions. Under the assumption that the structural design approach will ensure there will be additional safety reserve in the structural member capacity estimation, it is safe to assume that if the comparison between the codified load calculation and extreme load statistics can yield a reliability index greater than 3, the code formula is safe to be used. Table 4.3 lists the probability of exceedance and the reliability index of the design load calculation applied to both sites assuming different values of ice strength, considering a 75-year design life.

Table 4.6 Probability of Exceedance and Corresponding Reliability Index for 75-Year Design Life

	Probability of Exceedance, *p* (Reliability Index, β)*			
Effective Ice Strength (ksf)	8	16	24	32
James River Site with Reduction Factor	1 (NA)	1 (NA)	1 (NA)	0.98 (NA)
James River Site without Reduction Factor	1 (NA)	0.98 (NA)	0.0497 (1.6)	0.0014 (3.0)
Big Sioux River Site with Reduction Factor	1 (NA)	0.91 (NA)	0.086 (2.4)	6.9×10^{-5} (3.8)
Big Sioux River Site without Reduction Factor	0.91 (NA)	6.59×10^{-5} (3.8)	2.57×10^{-8} (5.4)	3.99×10^{-11} (6.5)

From the probability of failure analysis for the James River site presented in Table 4.3, it can be seen that, to be safe, one should use 32 ksf effective ice strength, with the ice thickness obtained from the USGS study ice thickness map, and without taking small stream reduction.

5. FINDINGS AND CONCLUSIONS

The ice load monitoring device custom-designed for this study achieved accurate load measurements in a laboratory environment. The on-site strain measurements of the device were affected by long-term temperature variations. However, this effect was removed by using a data filtering technique to identify dynamic impact events. The traditional strain gauge is temperature sensitive and can have poor fidelity over long duration. Given the opportunity in the future, researchers should consider other force measurement devices that are less sensitive to long-term environmental effects.
The on-site data collection and transmission system operated satisfactorily under harsh winter conditions to provide uninterrupted data. The protection measures applied during installation helped the system withstand winter and spring loading and debris conditions.

Measured ice strength from the sites over two years varied significantly, depending on temperature and ice condition. The maximum strength can reach greater than 600 psi during the middle of the winter. However, the measured ice crushing strength should not be directly used as the effective ice strength in the AASHTO LRFD Code design equations.

Ice impact loads at the sites can be fitted to a lognormal distribution. Based on the assumed annual number of impact events and basic statistics calculations, the 75-year maximum ice load for the James River site was calculated to have a median of 174.5 kips. The 75-year maximum ice load for the Big Sioux River site was calculated to have a median of 81.5 kips. Based on the comparison of the observed ice load statistics with the design calculations, the design using 222 psi (32 ksf) equivalent ice strength without the small stream reduction factor was found to provide a minimum reliability index of 3.0 for both sites.

6. RECOMMENDATIONS

6.1 Calculation of Ice Loads

The S.D. Department of Transportation should use an effective ice strength of 32 ksf, ice thickness as given in SD98-04-F, and no reduction for small streams for structural design.

For flows similar to the James and the Big Sioux rivers, we recommend that SDDOT use an effective ice strength of 32 ksf for small streams as listed in AASHTO LRFD Bridge Design Specifications and obtain the ice thickness from the ice thickness map contained in the SDDOT report "Estimation of Ice Thickness and Strength for Determination of Lateral Ice Loads on Bridge Substructures in South Dakota SD98-04-F." We also recommend that SDDOT should not consider the small stream reduction factor given in the AASHTO LRFD Bridge Design Specifications when calculating ice loads for flows similar to those that form on the James and the Big Sioux rivers.

These recommendations are based on the fact that using the ice thickness map data and 32 ksf effective ice strength together with the AASHTO LRFD Bridge Design Specifications requirements will generate design ice load values that result in a reliability index greater than 3.0 for both sites. This recommendation is based on the comparison between the AASHTO load calculation and the extreme ice load statistics derived from two-year monitoring data at the two selected sites. Although data are limited, the research team believes that the recommendation is on the safe side of AASHTO recommendations and is supported by existing data with reasonable reliability. Exclusion of ice dams and the limitation to small streams is in place because of the nature of the monitoring sites where data were generated.

6.2 Further Monitoring Efforts

The S.D. Department of Transportation should commission work to redesign the ice load monitoring system and collect data for at least five years from river sites that may induce more critical ice load conditions.

This recommendation is contingenton the need to conduct a comprehensive ice load calibration for South Dakota rivers. If there is no immediate need, this recommendation will not be applicable. If there is a need to perform this calibration, we recommend that SDDOT consider the possibility of conducting more data collection on ice impact load for a longer period of time (preferably more than five years) and at sites that cover more critical conditions (such as thick ice sheet floats and ice dams). The potential benefit of conducting this work is to develop an understanding of the realistic ice load demands in these locations and eventually correlate the ice load with weather and geographical data in South Dakota and developing a viable and scalable procedure for river ice load monitoring. Ideally the sites where ice impact damage was observed on bridge structures should be included. Based on experience from this project, the following modifications of the study plan should be implemented:

- The monitoring system should be redesigned with a focus on its sensitivity to long term temperature variations in an as-installed configuration (rather than only relying on the laboratory testing and calibration).
- Conduct the study in two phases. The first phase will only conduct field trial at limited sites, collect data for 1 to 2 years, and adjust the monitoring system design to yield satisfactory results. The second phase will replicate the validated system at multiple sites and collect data for a longer period (5 to 10 years).

- Supplement the ice load measurement with visual data, preferably using remote cameras to link the measurements with images reflecting river conditions.
- It will be beneficial to seek collaboration with other research entities that have the capacity to conduct scaled modeling or ice floe characterization, such as the US Army Cold Regions Research and Engineering Lab.

With the experience gathered and lessons learned from this study, it is likely that researchers can improve the current design and obtain better ice load data. The likelihood of success of the subsequent study depends on the plan for improving the monitoring device. If the existing sites can be used as test sites for the improved design before expanding the monitoring effort to other sites, the chance of getting improved quality data will be quite high.

REFERENCES

AASHTO, 2014, AASHTO LRFD Bridge Design Specifications with 2015 Interim Revisions, Seventh Edition, Washington DC.

Ahmed, D, 1994, Ice loads on conical piers: A finite element investigation, International Journal of Offshore and Polar Engineering, 4(1), pg: 53-61

Brown, T.G et al. (2010). Extreme Ice Load Events on the Confederation Bridge, Cold Regions Science and Technology, 60, pg: 1-14.

Brown, T. G., Tibbo, J. S., Tripathi, D., Obert, K., and Shrestha, N. (2009). "Extreme Ice Load Events on the Confederation Bridge." Cold Regions Science and Technology, Cold Regions Science and Technology 60, 1-14.

Frederking, RMW, Sayed, M., and Penney, G. 1992, Ice forces on light piers in the St. Lawrence Seaway, International Journal of Offshore and Polar Engineering, 2(1), pg: 67-72

Gerard, R. (1983). "River and Lake Ice Processes Relevant to Ice Loads." Design for Ice Forces: A State of the Practice Report, 121-138.

Haynes, F. D., Sodhi, D. S., Zabilansky, L. J., and Clark, C. H. (1991). "Ice Force Measurements on a Bridge Pier in the St. Regis River, New York." U.S. Army Corps of Engineers Cold Regions Research & Engineering Laboratory, Special Report 91-14, 1-6.

Jochmann P., Evers K., and Kuehnlein WL. 2003, Model testing of ice barriers used for reduction of design ice loads, Proceedings of 22nd International Conference on Offshore Mechanics and Arctic Engineering, Cancun, Mexico.

Lever J. and Gooch G. 2001, Design of Cazenovia Creek ice control structure, Journal of Cold Regions Engineering, 15(2), pg: 103-124

Montgomery, C. J., Gerard, R., Huiskamp, W. J., and Kornelsen, R. W. (1984). "Application of Ice Engineering to Bridge Design Standards." Canadian Society for Civil Engineering, 795-810.

Niehus, C. A. (2002). "Estimation of Ice Thickness and Strength for Determination of Lateral Ice Loads on Bridge Substructures in South Dakota." South Dakota Department of Transportation Office of Research, SD98-04-F, 1-64.

Timco GW., Nwogu OG., and Christensen FT., 1995, Compliant model tests with the Great Belt West Bridge piers in ice Part I: Test methods and key results, Cold Region Science and Technology, 23, pg: 149-164.

U.S. Geological Survey, 2002, Estimation of Ice Thickness and Strength for Determination of Lateral Ice Loads on Bridge Substructures in South Dakota, Technical Report SD98-04-F, September 2002.

Yuan Z., Yu T., and Zhang H., 2009, Research on percussive force of river ice and bridge, Proceedings of 2nd International Conference on Modeling and Simulation, Manchester, UK.